Article:
Zhi, D., Song, D., Chen, Y. et al. (2024) Spatial insights for sustainable transportation based on carbon emissions from multiple transport modes: A township-level case study in China. Cities: The International Journal of Urban Policy and Planning, 155. 105405. ISSN: 0264-2751

https://doi.org/10.1016/j.cities.2024.105405

Spatial insights for sustainable transportation based on carbon emissions from multiple transport modes: A township-level case study in China

Abstract

Understanding the CO_2 emissions and influencing factors of travelers' multiple modes can provide direction for energy conservation and emission reduction, which is of great significance for developing sustainable cities. Previous studies focused on the CO_2 emissions of the transportation sector or individual modes. which has overlooked the variations of emissions within the transport system. Hence, this study focuses on multiple modes (i.e., car, subway, bus, and bike) in the township in the Guangdong-Hong Kong-Macao Greater Bay Area. This study proposes a framework for exploring the spatial autocorrelation of urban transport emission structure based on ratios (i.e., CO_2 emissions from each mode divided by total emissions) and key factors by combining spatial econometric model (i.e., Moran's I index and Spatial Error Model) and machine learning model (i.e., Random Forest and SHAP model). In addition, the spatial autocorrelation of ratios at different spatial scales is investigated. The results indicate the high spatial dependence in the ratios from each transport mode and Moran's I indices for four ratios are 0.883, 0.886, 0.706, and 0.776, respectively. In addition, subway and car ratios exhibit a negative spatial correlation (-0.798), and subway and bike show a positive correlation (0.570). Population density, road length, and land use diversity are the key drivers of CO_2 emission ratios and have different effects on various transport modes. Furthermore, as the spatial scales expand from townships to distinct and city, the spatial autocorrelation of the ratios decreases. This study could provide policy implications for optimizing urban transport strategies and reducing CO_2 emissions.

Keywords

CO_2 emissions; Traffic emission structure; Multiple transport modes; Spatial

correlation; Spatial error model; SHAP

1. Introduction

The transport sector is facing increasing challenges in today's world. As urbanization accelerates and economic development continues to advance, the negative impacts of traditional transport modes are becoming increasingly evident (Mahmoudi et al., 2019). Air pollution caused by vehicle emissions, time wastage caused by traffic congestion, and casualties and property damage caused by traffic accidents have all become important factors restricting the sustainable development of society. Against this backdrop, sustainable transportation has attracted much attention as an emerging development paradigm. The sustainability of transportation is defined in three main dimensions: social, economic, and environmental (Mahmoudi and Rasti-Barzoki, 2018; Mahmoudi et al., 2019). To limit temperature change to below 2 degrees Celsius, the world will need to transition to near-zero emissions across the global energy system by no later than 2060, the environmental dimension of sustainable transport has received increasing attention (Allen, 2018). Urban agglomerations, the highest spatial organization form of urban development, are multi-level urban unions formed by the agglomeration of several large cities and mega-cities distributed geographically (Wang et al. 2020). Meanwhile, it was also shown that China’s carbon emissions primarily concentrate in urban agglomerations (Qian et al. 2022). Hence, it is necessary to pay attention to emission reduction policies for urban agglomerations with increased carbon emissions in the context of carbon peaking and neutrality (Liu and Xiao 2018, Wang et al. 2020).

The reliance of transportation on fossil fuels and the inefficient use of transportation systems have resulted in significant emissions of carbon dioxide (CO_2), playing a role in global climate change. Transportation contributes to over 20% of global energy-related CO_2 emissions, and this number is expected to double by 2050 (Xia et al., 2023). Therefore, the development of policies to control traffic CO_2 emissions has become a key problem that urgently needs to be resolved. Exploring the

establishment of a sustainable transport system requires a focus on the CO_2 emissions of various modes. Assessing the CO_2 emissions of different transport modes helps identify the predominant contributor, facilitating the formulation of energy-saving and emission-reduction policies for sustainable transportation (Liu et al., 2023). Additionally, analyzing the relationships between various transport modes, particularly in terms of spatial competition or collaboration, inspires spatial multimodal coordination to enhance traffic efficiency and consequently reduce emissions (Becker et al., 2022; Deng et al., 2022).

While previous studies have explored CO_2 emissions of the transport system from a spatial perspective, they often focused on large-scale aggregate levels, e.g., country level (Lin et al., 2019; Liu et al., 2022; Zhu, 2023), province level (Bai et al., 2019; Liu et al., 2022; Ma et al., 2022), and city level (Sun et al., 2017; Gao et al., 2022; Liu et al., 2023). Large-scale aggregated studies may fall short of providing the necessary granularity to capture variations in CO_2 emissions at a smaller scale. However, to the best of our knowledge, studies on transport CO_2 emissions at the fine-grained township level are still scarce, which leaves a gap in understanding the CO_2 emission of transportation systems from a more detailed spatial perspective. In addition, previous studies focused on the CO_2 emissions of a specific individual transport mode or the whole transportation sector, e.g., passenger transportation sectors (He et al., 2013; Batur et al., 2019; Liu et al., 2023), car (González et al., 2019; Türe and Türe, 2020), public transport (García-Cerrud et al., 2021; García-Afonso, 2023; Dasgupta et al., 2023) and bike (McQueen et al., 2020). However, there is a lack of research on the CO_2 emissions of various transport modes within the transportation system, especially from the spatial perspective. Examining the CO_2 emissions of individual transport modes, while valuable, presents limitations. Focusing solely on a single mode neglects the intricate interactions and complexities within the entire transportation system. This approach may fail to comprehensively assess the overall CO_2 footprint when various modes are used in combination. Hence, studying the spatial patterns and influencing factors of

CO_2 emissions from various transport modes is imperative. This study could enable a holistic understanding of how emissions vary across different geographic locations and transport modes, providing crucial insights for developing effective strategies to reduce carbon emissions and promote sustainability across diverse modes of transportation.

Furthermore, previous studies about traffic CO_2 emissions mostly analyzed the influencing factors from the single perspective of spatial metrology or machine learning, lacking the framework of coupling the spatial econometric model and machine learning model. CO_2 emissions often exhibit significant spatial dependence, meaning that the emission levels in one area can be influenced by those in neighboring areas. Spatial econometric models can effectively capture these spatial relationships, revealing the interactions and spillover effects of emissions between different regions. In detail, spatial econometric models such as the Spatial Durbin Model and the Spatial autoregressive model have been widely applied to study the drivers of traffic CO_2 emissions (Lv et al., 2019; Song et al., 2021). Due to the powerful ability of machine learning to capture nonlinear relationships, the application of these models has grown significantly, leading to numerous studies that utilize these models to predict CO_2 emissions. (Ağbulut 2022; Sahraei and Çodur, 2022; Javanmard et al., 2023; Khajavi and Rastgoo, 2023). Compared to this literature on CO_2 prediction using machine learning, there are few studies that use interpretable machine learning models to reveal the complex relationships involved (Qiao et al., 2024; Zhi et al., 2024).

To sum up, studies on understanding CO_2 emission of multiple transport modes from a spatial perspective at fine-grained spatial scales are still scarce. Compared to individual transport modes, examining the CO_2 emissions of multiple transport modes allows for a deeper understanding of the underlying behavioral factors that drive human choices of different transport modes and the urban transport emission structure. This understanding can inform the development of behavior-oriented policies to encourage more environmentally friendly travel behavior to minimize CO_2 emissions. Meanwhile, exploring the relationship between CO_2 emissions from multiple modes of

transportation from spatial and nonlinear perspectives can help to discover patterns of competition or collaboration among transport modes across different geographic regions. This analysis can provide valuable insights into how these modes interact, which can inform strategies to enhance synergies, improve overall travel efficiency, and ultimately reduce carbon emissions. Moreover, the study of fine-grained CO_2 emissions from various modes of transport on a more detailed spatial scale is helpful for governments to make precise and locally tailored policies on CO_2 emissions from transport systems.

To fill the gap, this study aims to explore the spatial correlation and influencing factors of CO_2 emission from multiple transport modes, including cars, subways, buses, and bikes, based on the township-level data in an urban agglomeration (i.e., Guangdong-Hong Kong-Macao Greater Bay Area (GBA)). Firstly, Moran's I index is used to analyze the spatial correlation of the CO_2 emission ratio for each transport mode and each pair of modes, respectively. Secondly, the influencing factors based on the "4D" principle (Density, Distance, Diversity, and Design) are examined. Then the framework combining the SEM and interpretable machine learning models is proposed to quantify the relationships between these factors and the CO_2 emission ratios (i.e., urban transport emission structure) of the four modes. Furthermore, the spatial correlations of transport mode ratios across different spatial scales, ranging from township to district and city levels, are explored. The findings of this study can provide valuable insights into the spatial patterns of CO_2 emission from multiple transport modes. By identifying the key drivers of emissions, policymakers can prioritize interventions to mitigate CO_2 in areas with a high impact.

In summary, the main contribution of this study is to investigate the spatial relationship between the CO_2 emission ratios of various transport modes and the corresponding influencing factors in the GBA. Specific contributions are as follows:

(1) Focus on the urban transport emissions structure based on four transport modes and reveal the spatial differences and connections of the CO_2 emission ratio of

different modes at the township level in urban agglomerations.

(2) Explore the influence of factors on the CO_2 emission ratio of different transport modes by using the framework combining the SEM model and interpretable machine learning models, which can reveal spatial and nonlinear relations.

(3) Uncover the differences in the spatial correlation of CO_2 emission ratio across multiple transport modes at different spatial scales in the urban agglomeration, providing insights into how spatial patterns of ratios evolve across scales.

The rest of this research is structured as follows: **Section 2** provides an overview of the related works. **Section 3** explains methodologies. **Section 4** presents the model results. **Section 5** provides a discussion. **Section 6** outlines the policy implications. Finally, **Section 7** summarizes the key findings and further studies.

2. Related works

Regarding sustainable transportation, the social, economic, and environmental dimensions have been the subject of much previous research. Among them, studies on the social dimension in sustainable transport mostly focus on accessibility to employment, accessibility to major public services, spatial equity, community cohesion, safety, transportation variety, traffic congestion, comfort of public transportation (Iniestra and Gutiérrez 2009; Haghshenas et al. 2015; de Almeida Guimarães and Leal Junior 2017; Mansourianfar and Haghshenas 2018; Oses et al. 2018; Karamanlis et al., 2023). Regarding the economic dimension of sustainable transportation, previous studies have mainly concerned with travel time, global surplus, employment evolution, travel cost, transportation cost for the government, indirect transportation cost for the user, economic development, and urban economic resilience (Basbas and Politis 2008; Joumard and Nicolas 2010; Haghshenas et al. 2015; Mansourianfar and Haghshenas 2018; Li et al., 2023). Many studies are focusing on the environmental dimension of sustainable transportation. The topics of these studies include but are not limited to biodiversity and protected sectors, GHG emissions, local air quality, noise pollution,

energy use, water pollution, space/land consumption, consumption of non-renewable materials (Basbas and Politis, 2008; Nanaki et al., 2017; Nadafianshahamabadi, Tayarani, and Rowangould, 2017; Oses et al., 2018; Mansourianfar and Haghshenas 2018; Qiao and Huang, 2022; Sun et al., 2024). With the worldwide concern about climate warming, many studies focus on emissions in the environmental dimension of sustainable transport. Considering the urgency of reducing carbon emissions, our study focuses on the environmental dimensions of sustainable transportation.

2.1 Exploration of CO_2 emission from transportation

This subsection organizes and summarizes the work related to the CO_2 emission of transportation in Table 1. Most of the current research focuses on CO_2 emission from the whole transport sector, mainly analyzing the drivers at different spatial scales, including the country-, province-, and city-level (Zhu et al., 2019; Liu et al., 2021; Lv et al., 2019; Song et al., 2021; Zhi et al., 2024). These emission data are generally provided by the government or environmental component statistics. There are fewer studies on CO_2 emissions from the whole transport sector at scales smaller than the city, probably because whole emissions at fine scales are difficult to calculate and obtain. In addition to focusing on emissions from the transport sector as a whole, some studies focus on CO_2 emissions from passenger and freight transport separately (He et al., 2013; Liu et al., 2017; Xu et al., 2021; Liu et al., 2023). The emissions in these studies are generally quantified by the researchers themselves. For example, Liu et al (2023) introduced a technique for estimating and studying CO_2 emissions from urban passenger transportation using sparse trip trajectory data. Their approach involved constructing a multi-scale platform for calculating and monitoring transportation CO_2 emissions, utilizing a bottom-up calculation method. This platform could assess the CO_2 emissions across various passenger transportation modes, including walking, cycling, buses, metro, and cars. Moreover, a great number of studies focus on the CO_2 emissions of single transport modes, including cycling, subway, buses, and bike-sharing

(González et al., 2019; Türe and Türe 2020; Kou et al., 2020; García et al., 2022a; García et al., 2022b; Zhi et al., 2022; Dasgupt et al., 2023). Specifically, Li and Yu, (2019) assessed peaking CO_2 emissions of urban passenger transportation sectors in China. Other studies explored car-related CO_2 emissions (González et al., 2019; Türe and Türe, 2020). For example, González et al., (2019) examined the evolving correlation among CO_2 emissions from cars in Western European Union countries between 1990 and 2015. There is also a large body of literature concerned with the CO_2 emissions of public transport, especially buses, and subways (Liu et al., 2018; García-Cerrud et al., 2021; Dasgupta et al., 2023; García-Afonso, 2023). In addition, there are also some studies on estimating CO_2 emissions from e-bikes and bikes (Chen et al., 2020; McQueen et al., 2020; Zhi et al., 2021). A common methodology used in these studies is life cycle assessment modeling, especially for emerging transport modes or new energy buses (Kou et al., 2020; García et al., 2022a; Zhi et al., 2022). Although some studies have quantified the CO_2 value from multiple modes, they have not explored their relationship (Liu et al., 2017; Liu et al., 2023).

As shown above, there has been a lot of research on CO_2 emissions from the whole transport sector, passenger, freight, and individual transport modes. However, there is a gap in exploring and comparing the CO_2 emission from multiple transport modes from a spatial perspective. In addition, previous studies have paid little attention to spatial scales smaller than the city (e.g., the township level), and even less to township-level studies of urban agglomerations of significance.

There are three main categories of methods to explore the factors influencing traffic CO_2: decomposition analysis methods, spatial econometric models, and machine learning models, and, as shown in Table 1. Among the decomposition analysis methods, the Logarithmic Mean Divisia Index is mainly used for macro-level studies and is less concerned with fine-grained spatial analyses (Liu et al., 2021). Spatial econometric models are mainly based on linear assumptions to deal with spatial dependence. Regarding the spatial econometric models, the Spatial Durbin Model can effectively

capture spatial dependence and spillover effects and is suitable for the study of inter-regional interactions (Lv et al., 2019). The spatial autoregressive model effectively reveals the spatial dependence between regions (Song et al., 2021). Both studies in the table combine machine learning models and post-interpretation models to reveal the nonlinear relationship between traffic CO_2 and influencing factors in depth (Qiao et al., 2024; Zhi et al., 2024). For example, Qiao et al. (2024) developed an interpretable multi-stage forecasting framework for quantifying CO_2 emissions in the UK's transport sector. This framework uses diverse input features from socioeconomic, transportation, and energy-related sources. It integrates interpretable machine learning methods with the SHapley Additive exPlanations (SHAP) technique to enhance forecasting accuracy and reveal the relationships between predictions and key influencing factors.

In summary, there is a lack of comparative studies focusing on CO_2 emission of multiple modes from a spatial and nonlinear perspective by combining spatial econometric models and interpretable machine learning models. Gaining insights into the spatial patterns of CO_2 emissions enables enhanced design of transportation infrastructure and the optimization of transport networks. This understanding facilitates strategic planning that encourages the adoption of low-carbon modes, promoting sustainable and environmentally friendly transportation practices.

Table 1. Summary of related works

Literature	Study object	Research topic	Study area	Study unit	Method	**Multiple transport modes**	**Incor porat**

						Include?	From a spatial perspective?	**ing different methods**
Liu et al. (2021)	CO_2 of the whole transport sector	Influencing factor of the traffic CO_2 emission	China	Country Level	Logarithmic Mean Divisia Index	×	×	×
Lv et al. (2019)			China	Province Level	Spatial Durbin Model	×	×	×
Song et al. (2021)			China	City Level	Spatial autoregressive model	×	×	×
Zhi et al., (2024)			China		Machine learning	×	×	×
Qiao et al (2024)			UK	Country Level	Machine learning	×	×	×
Xu et al.(2021)	Truck emissions between cities	Calculating CO_2 emissions from freight transportation	Beijing-Tianjin-Hebei urban agglomeration	City Level	Gravity theory	×	×	×
He et al.(2013)	The urban passenger transportation sector	Calculating CO_2 emissions from passenger transportation	China	City Level	Bottom-up CO_2 emissions calculation approach	×	×	×
Liu et al. (2017)	CO_2 emissions of urban motor and metro transports		Wuhan	Subdistrict and town		√	×	×
Liu et al.(2023)	CO_2 emissions from walking, cycling, buses, metro, and cars		Hangzhou	Road Level		√	×	×
González et al. (2019)	Passenger cars' CO_2 emission	Influencing factor of cars' CO_2 emission	Europe	Country Level	Dynamic Panel Data model	×	×	×
Türe and Türe (2020)			Europe	/	Mathematical modeling	×	×	×
Dasgupt et al(2023)	CO_2 emission related to subway	Impact of the subway on CO_2	World	Functional urban areas	Global emissions model,	×	×	×
García et al. (2022a)	CO_2 of bus	Calculating CO_2 emissions from bus	Spain	City Level	Life cycle assessment	×	×	×
García et al. (2022b)		Pathways to reduce CO_2 emission for bus transit networks	Spain	/	Simulation method	×	×	×

Kou et al., (2020)	CO_2 of bike-sharing	Calculating CO_2 emissions from bike-sharing system	United States	City Level	Life cycle assessment	×	×	×
Zhi et al., (2022)			China and the United States	City Level	Life cycle assessment	×	×	×
This study	**CO_2 emissions from cars, subways, buses, and bikes**	**Spatial pattern and influencing factor of CO_2 emission of four transport modes**	**GBA (urban agglomeration)**	**Township Level; District Level; City Level**	**A methodological framework for integrating SEM and interpretable machine learning models**	√	√	√

2.2 Gap analysis

Despite extensive research on CO_2 emissions across various scales (country, province, city) and for individual transport modes (cars, buses, subways), there is a notable gap in studies that examine CO_2 emissions from multiple transport modes simultaneously from a spatial perspective. Existing research often focuses either on aggregate levels or on single transport modes, overlooking the interactions and spatial relationships between different modes. Additionally, fine-grained spatial scales, such as the township level within urban agglomerations, are underexplored. This limitation hampers understanding of how different transport modes interact spatially and their combined impact on CO_2 emissions.

Moreover, current methods for analyzing traffic CO_2 emissions predominantly rely on linear spatial econometric models, which effectively capture spatial dependencies but fall short in addressing complex nonlinear relationships. While spatial econometric models like the Spatial Durbin Model and spatial autoregressive models provide valuable insights into spatial interactions, they do not fully capture nonlinear dynamics. Conversely, although machine learning techniques offer advanced capabilities for modeling nonlinear relationships, they are often used separately from spatial analysis. There is a lack of integrated approaches that combine spatial econometric models with interpretable machine learning methods to comprehensively address both spatial and

nonlinear aspects of CO_2 emissions.

Therefore, this study focuses on multiple transport modes to explore the spatial differences and linkages in their CO_2 emissions and influencing factors. Given that the GBA is one of the most important urban agglomerations in China and covers a wide range of city types, with strong transport links between cities, it is chosen as the study area. The four transport modes of car, subway, bus, and bike are primarily responsible for intra-city travel, and studying CO_2 emissions from these modes on the township level is useful for capturing finer-grained features. This study aims to propose a framework for quantifying impact considering the spatial and nonlinear relationship between CO_2 emissions and influencing factors.

3. **Methodology**

3.1 Data description and research framework

Urban agglomerations are a highly spatialized form of organization in which urban development has come to maturity. (Xu et al., 2021). As an important internationalized urban agglomeration in China, the CO_2 status from the transportation of the GBA has a significant impact on the achievement of China's overall carbon reduction targets. In this study, the research region is GBA, including 9 cities and 2 special administrative regions (i.e. Hong Kong and Macau), as shown in Figure 1. The 630 township-level areas in the GBA are selected in the study, as shown in each city or special administrative region in this figure.

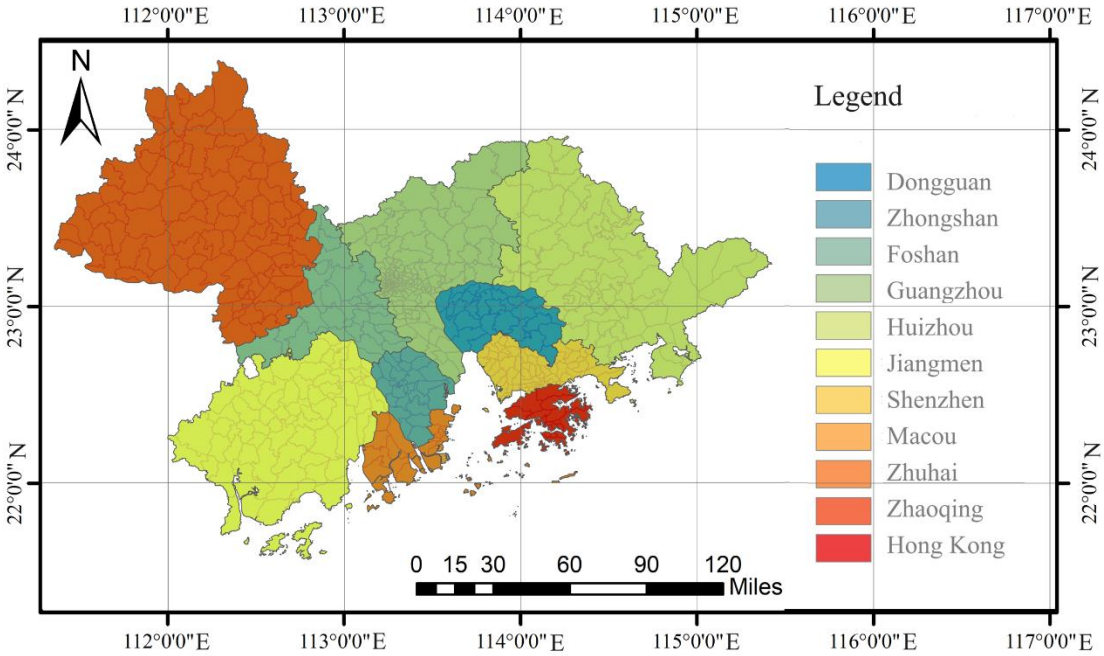

Figure 1. Administrative divisions at the city and township level in the GBA

The studied data are obtained from the cooperating company and provide information on the CO_2 emission of the four transport modes (i.e., car, subway, bus, and bike) for a full year in 2021. In addition, this data does not include emissions associated with motorcycles. The CO_2 emissions for each mode are obtained by using the traveler's trajectory data. Table 2 shows the sample data on CO_2 emission from the four transport modes in the townships of the GBA.

Table 2. Sample data of CO_2 emission from the four transport modes (unit: kg)

Township ID	Car	Subway	Bus	Bike
440785104	1094086.526	180811.492	456704.142	9056.764
440785108	1357566.371	213567.418	619698.667	10232.108
440785106	1395204.313	232020.191	574815.140	9725.901
440785102	1130591.792	180697.816	540276.656	11337.944
440785100	1642765.412	257239.415	734362.517	11471.460

The size and traffic conditions of different townships can vary considerably, resulting in CO_2 emission in absolute terms not being directly comparable. The study calculates the ratios of CO_2 emission from the four modes of transport in each town to

make it more comparable between different townships. The calculated ratios are named as Car-Ratio, Subway-Ratio, Bus-Ratio, and Bike-Ratio, the mean values are 60.01%, 12.84%, 26.33%, and 0.72%, respectively. These ratios reflect the urban transport emission structure. Figure 2 presents 3D plots of these four CO_2 emission ratios, indicating their spatial heterogeneity and correlation. The height of the townships in the figure corresponds to the absolute value of CO_2 emissions shown in Table 2, and the color corresponds to the value of the "Ratio". From the figure, it can be seen that the distribution of CO_2 emissions with respect to "Ratio" is not consistent.

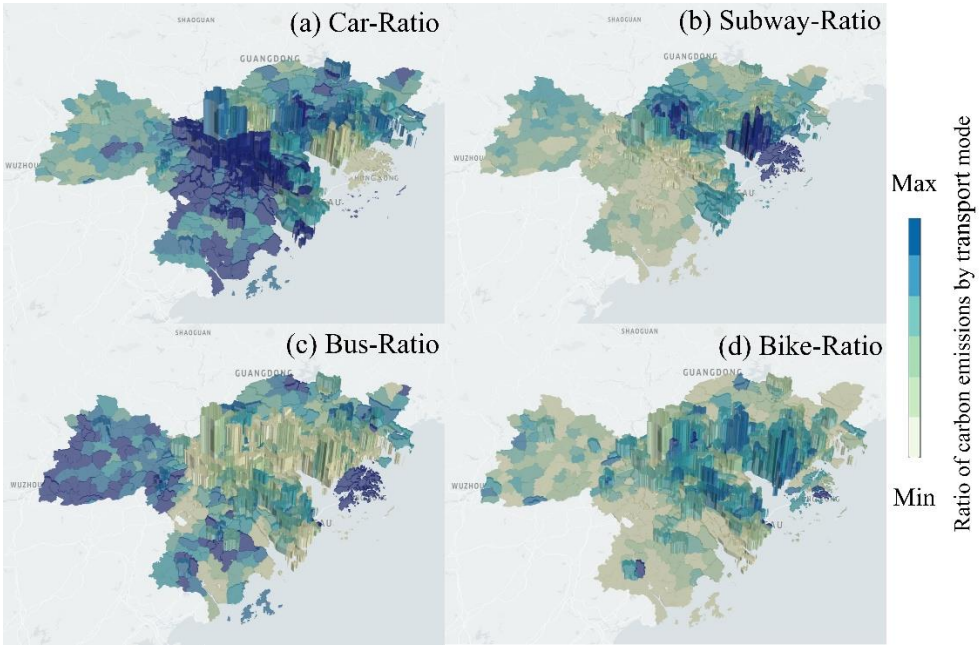

Figure 2. Illustration of CO_2 emission ratios of four transport modes in each township

The objective of this research is to examine the spatial patterns of CO_2 emissions from travelers using the same mode across various townships, as well as those using different multiple transport modes. Based on the fine-grained township-level data on CO_2 emission from four transport modes (i.e., bike, bus, subway, and car), this study first explores the spatial correlation of the CO_2 emission ratios of transport modes, which involves computing the global Moran's I index of CO_2 emission ratios for individual transport modes and each pair of two transport modes. Then, based on the features selected by the "4D" principle, SEM considering spatial spillover effects is

used to explore the drivers of CO_2 emission ratios of different transport modes. To further quantify the contribution of each feature, the machine learning model Random Forest and post-interpretation model SHAP are combined for analysis. Finally, the changes in the spatial correlation of the CO_2 emission ratios of transport modes at different spatial scales are compared. The framework diagram of this study is shown in Figure 3.

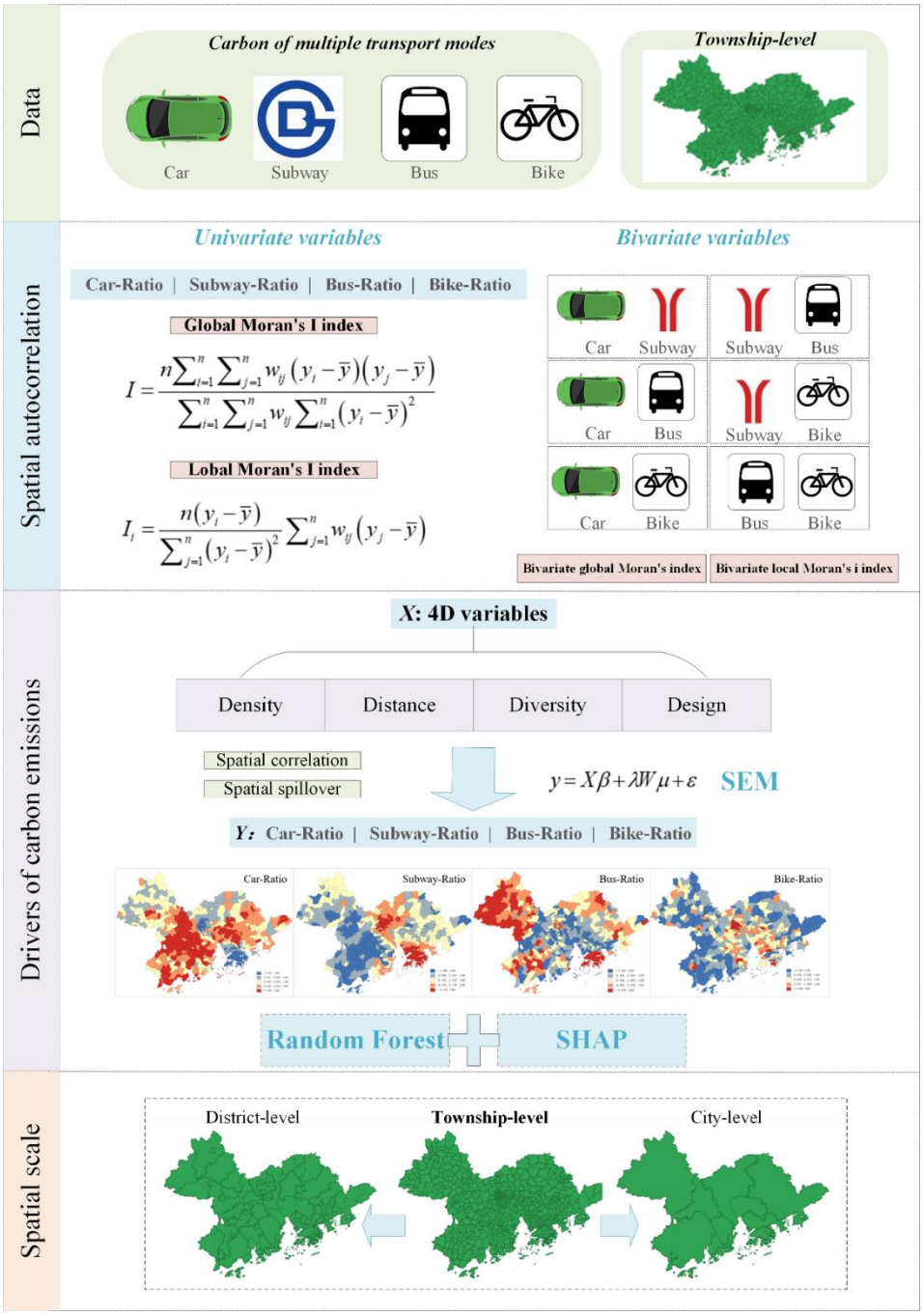

Figure 3. The framework diagram for this study

3.2 Spatial autocorrelation of CO_2 emission ratio of individual transport modes

To explore the spatial mobility of CO_2 emission of individual transport modes, global and local Moran's I indices are employed to measure the spatial autocorrelation of CO2 emission ratios of each transport mode, as follows.

3.2.1. Global effects of CO_2 emissions from individual transport modes

Global Moran's I test is widely employed as a spatial variability test, which can provide insights into the spatial autocorrelation of the CO_2 emission ratio of each transport mode (Moran 1950; O'sullivan and Unwin, 2003; Srejic et al., 2023). Global Moran's I is a commonly used indicator for measuring the spatial patterns of geographical phenomena, which is presented in the following manner according to Moran (1950):

$$I = \frac{n\sum_{i=1}^{n}\sum_{j=1}^{n} w_{ij}\left(y_i - \bar{y}\right)\left(y_j - \bar{y}\right)}{\sum_{i=1}^{n}\sum_{j=1}^{n} w_{ij}\sum_{i=1}^{n}\left(y_i - \bar{y}\right)^2} \quad (1)$$

where n is the number of studied townships. w_{ij} is the weight between townships i and j. y_i and y_j are the CO_2 emission ratios of the same transport mode at townships i and j, respectively. $\bar{y}$ is the average value of ratios in all townships.

The global Moran's I indices range from -1 to 1, reflecting different spatial patterns. Positive values indicate spatial aggregation, meaning that close townships tend to have similar CO_2 emission ratios while distant townships have different ratios. Conversely, negative values indicate spatial dispersion, suggesting that observations are more dissimilar as distance increases. A value near 0 indicates a spatially random distribution, where no clear spatial pattern can be discerned. The significance of the Moran's I statistic is typically assessed using a Z-score, as follows (Moran, 1950; Ma et al., 2020):

$$Z(I)=\frac{I-E(I)}{\sqrt{Var(I)}} \tag{2}$$

where $E(I)$ represents the expected value of the global Moran's I statistic. $Var(I)$ represents the standard deviation. The significance level in township-level data is set as $P<0.001$.

3.2.2. Lobal effects of CO_2 emissions from individual transport modes

Local Moran's I serves as the decomposed version of the global Moran's I, allowing for a more detailed examination of the spatial agglomeration characteristics of individual townships and the identification of hotspots through comparisons with neighboring areas (Anselin, 1995; Zhang et al., 2008). The computational equation is presented as follows (Zhang et al., 2008).

$$I_i=\frac{n(y_i-\bar{y})}{\sum_{j=1}^{n}(y_i-\bar{y})^2}\sum_{j=1}^{n}w_{ij}(y_j-\bar{y}) \tag{3}$$

where n, y_i, y_j, y and w_{ij} are identical to the terms in Eq. (1).

Additionally, the results of the computed local Moran's I indices are visualized through the Local Indicators of Spatial Association (LISA) cluster map, helping us detect CO_2 ratio clusters and outliers in the study area (Wang et al., 2020b).

3.3 Spatial correlation of CO_2 emission ratio of bivariate transport modes

To investigate the spatial relationship between the CO_2 ratios of two transport modes, the bivariate Moran's I index for each pair of modes among the four transport modes is calculated, resulting in a total of 12 sets of Moran's I values ($A_4^2=12$). The computation of bivariate Moran's I index is shown below.

3.3.1. Global effects of CO_2 emissions from bivariate transport modes

While spatial autocorrelation above describes geographic elements with only one

variable, bivariate-based spatial autocorrelation has high applicability and validity in describing the spatial association and dependence characteristics of two geographic elements. Hence, the bivariate Moran's I index, an enhanced iteration of the traditional Moran's I index, serves as a spatial autocorrelation measure to assess the spatial relationship between two transport modes' CO_2 emission ratios (Srejic et al., 2023). Similar to Moran's I of individual transport modes' ratio, bivariate Moran's I statistics come in two forms: global and local. The global bivariate Moran's I provide an overview of the spatial relationship of two ratios of different modes across all townships throughout the entire GBA. It can be computed using the following equation (Moran, 1950; Gao et al., 2022).

$$I^{ab} = \frac{\sum_{i=1}^{n}\sum_{j=1}^{n} w_{ij}\left(y_i^a - \overline{y}^b\right)}{S^2 \sum_{i=1}^{n}\sum_{j=1}^{n} w_{ij}} \tag{4}$$

where y_i^a is the standardized CO_2 emission ratio of transport mode *a* in township *i*. $\overline{y}^b$ is the average CO_2 emission ratio of transport mode *b*. S^2 is stand for the variances of the ratios for the transport mode *a*. The ratios of transport modes *a* and *b* are selected from Car-Ratio, Subway-Ratio, Bus-Ratio, and Bike-Ratio.

The bivariate Moran's I index is employed to measure the spatial correlation between each pair of two transport modes. Its value ranges from -1 to 1. The type and strength of spatial correlation can be interpreted by the positive or negative sign and the magnitude of the value. If the value of the bivariate Moran's I index is close to 1, it means that the CO_2 emissions ratios of two different transport modes show a positive spatial correlation. This means that when the value of one CO_2 emission ratio is higher in a particular township, the value of the other ratio is also higher in the townships adjacent to it and vice versa. Conversely, if the value of the bivariate Moran's I index is close to -1, it means that the two ratios show a negative spatial correlation. This means that when the value of one ratio is higher in one township, the value of the other ratio is lower in the townships adjacent to it and vice versa. (Gao et al., 2022).

3.3.2. Local effects of CO_2 emissions from bivariate transport modes

The bivariate local indicator of spatial autocorrelation for variables *a* and *b* is a widely used method for assessing spatial heterogeneity and identifying local clusters (Aturinde et al., 2019; Gao et al., 2022).

$$I_i^{ab} = \frac{n\left(y_i^a - \overline{y}^a\right)}{S_a^2} \sum_{j=1}^{n} w_{ij} \frac{y_j^b - \overline{y}^b}{S_b^2} \tag{5}$$

where $\overline{y}^a$ is the average CO_2 emissions ratio of transport mode *a*. y_j^b is the standardized CO_2 emissions ratio of transport mode *b* in township *j*. S_a^2 and S_b^2 are stand for the variances of the ratios for the transport modes *a* and *b*, respectively.

3.4 Spatial error model

In this study, SEM is employed to quantify the impact of factors on the CO_2 emission ratios of different transport modes. The selection of SEM is based on two tests, i.e., the Lagrange Multiplier (LM) test and the Likelihood Ratio (LR) test (Elhorst, 2014). The specific results of the two tests are in subsection 4.3. Based on the results of two tests, considering the interactions and dependencies between spatially adjacent areas, the SEM is employed to explore how the driving factors (i.e., explanatory variables) influence the CO_2 emission ratios of four transport modes in township regions. By applying the SEM, the spatial spillover effects are considered and traditional econometric models are extended by incorporating spatial relationships and spatially lagged variables. This allows for the investigation of spatial patterns, spatial spillover effects, and the impact of neighboring observations on the dependent variable. In the SEM model, the dependent variable of any township is influenced not only by its independent variables but also by the errors of neighboring townships (Ibeas et al., 2012):

$$y = X\beta + \lambda W\mu + \varepsilon \tag{6}$$

where *y* can be Car-Ratio, Subway-Ratio, Bus-Ratio, and Bike-Ratio. *X* is the

explanatory variable. β is the estimated parameters related to diverting variables. λ is a spatial autocorrelation parameter of errors. W represents a matrix of spatial weightings. μ represents the spatial error term. ε represents the interference term.

Then, the explanatory variables (i.e., built environment indicators) influencing CO_2 ratios are selected based on the "4D" (density, distance, diversity, design) principles, which is an essential approach to understanding the intricate relationship between township form and CO_2 emission (Tu et al., 2021; An et al., 2022; Gao et al., 2023). **Density** measures the concentration of activities and population, **distance** captures the spatial accessibility, **diversity** accounts for the variety of land uses, and **design** encompasses the physical layout of the road network. By considering these variables, the spatial, social, and design factors that contribute to CO_2 of transport modes can be analyzed comprehensively. The specific variables selected and their meanings are summarized in Table 3. The variables with a variance inflation factor (VIF) score greater than 10 are excluded, as recommended in the literature (Taiebat et al., 2022). The VIF values of the variables are provided in **Appendix B**. In addition, the selection of explanatory variables is based on an ablation study, and the variables that have a significant impact on the accuracy of the model are selected. In ablation studies, researchers gradually remove certain parts or features of the model and then observe changes in model performance to understand the importance of each component to the model and how they interact with each other (Girshick et al., 2014).

Table 3. The description of explanatory variables

Type	Variables	Description
Density	POP	The population density in 2021
	Residence	The density of residences POI
	Mall	The density of mall POI
	Hotel	The density of hotel POI
	Factory	The density of factory POI
	Bus station	The density of bus stations POI
	School	The density of school POI
	Office building	The density of office buildings POI

	Restaurant	The density of restaurants POI
	Subway station	The density of subway stations POI
Distance	Center-distance	Straight line distance from the center (unit: km)
Diversity	Land use diversity	The entropy of all types of POIs in the service area
Design	Trunk	The total length of the trunk divided by the area of the township (unit: km)
	Tertiary	The total length of tertiary divided by the area of the township (unit: km)
	Secondary	The total length of the secondary divided by the area of the township (unit: km)
	Primary	The total length of the primary divided by the area of the township (unit: km)
	Motorway	The total length of the motorway divided by the area of the township (unit: km)

3.5 Machine learning models

Considering the advantages of machine learning from various perspectives, this study incorporates machine learning into the analytical framework. Specifically: (a) Machine learning excels at fitting complex nonlinear relationships with high accuracy (Qiao et al., 2024). (b) Although machine learning models previously faced issues with interpretability, recent methods such as SHAP and ALE now offer ways to explain model results (Zhi et al., 2024). (c) While SEM analysis has provided coefficients for influencing factors, these coefficients alone are insufficient for revealing the relationship between different samples and CO_2 emission ratios. Interpretative machine learning models can address this limitation.

Inspired by Bai et al (2023) 's incorporation of spatial information into machine learning models, this study couples the SEM model with machine learning models to further quantify the impact of explanatory variables on the CO_2 emission ratio. The specific steps are as follows:

Step 1 Extracting explanatory variable of machine learning models based on SEM fitting results

The parameters β and λ in Equation (6) can be obtained by fitting the relationship between the explanatory variables and the four ratios (i.e., Car-Ratio,

Subway-Ratio, Bus-Ratio, and Bike-Ratio) using SEM. Therefore, based on obtaining the parameters of Equation (6), the explanatory variables can be input into SEM to obtain the predicted values $\hat{y}_{SEM}$, and furthermore to obtain the residuals (i.e., SEM_residuals) $\Delta y_{SEM} = \hat{y}_{SEM} - y^*$ between the predicted values and the true values y^*. SEM_residuals take into account the geospatial correlation. Generally, environmental, economic or social factors may be similar between neighboring regions, so their residuals may show certain spatial patterns or correlations. To capture the effect of SEM_residuals Δy_{SEM} on the four ratios, it is added to the explanatory variables in Table 3. This new dataset of explanatory variables will be fed into the machine learning model to further explain its effect on carbon emission ratios.

Step 2 Relationship construction based on regression model Random Forest

Random Forest is among the most accurate general-purpose classifiers so far with the capability of handling high dimensional data (Biau, 2012; Yan et al., 2020). Random forest is essentially a tree-based ensemble method: it trains multiple decision trees and combines the predictions of all the decision trees to generate a final prediction (Breiman, 2001). In this study, the Random Forest model, built using the Python library scikit-learn, is tuned with grid search to select a candidate model with 1000 decision trees.

The dataset includes 630 samples (i.e., 630 townships), each with 18 explanatory variables x_i—one more than the 17 listed in Table 3. For each township, there are corresponding explained variables y_i (i.e., actual Car-Ratio, Subway-Ratio, Bus-Ratio, and Bike-Ratio). The selected Random Forecast model predicts the corresponding Ratio $\hat{y}_i^{RF}$ using these explanatory variables.

Step 3 Relationship interpretation based on the SHAP model

Input the predicted values (i.e., $\hat{y}_i^{RF}$) of all the townships, obtained from the trained Random Forecast, along with the corresponding explanatory variables (i.e., x_i), into the SHAP model. SHAP aims to interpret model predictions by quantifying the contribution of each explanatory variable. Specifically, the contribution of a given explanatory variable *i*, known as its SHAP value ϕ_i, can be determined using the following method (Molnar, 2020):

$$\phi_i = \sum_{S \in E \setminus \{i\}} \frac{|S|!(M-|S|-1)!}{M!} \left[f\left(S \cup \{i\}\right) - f\left(S\right) \right] \quad (7)$$

where E is the set of all input explanatory variables. S is the set of non-zero indexes in z', and z_i' represents variable i being observed ($z_i' = 1$) or not ($z_i' = 0$). $f\left(S\right)$ is the expectation of the function conditioned on subset S. $|S|$ and M are the numbers of variables in subset S and set E, respectively.

4. Result analysis

4.1 Spatial autocorrelation of univariate modes for CO_2 emission ratios

As described in **Section 3.2**, the spatial correlation of the CO_2 emission ratios from the four modes in each township is calculated, i.e., Car-Ratio, Subway-Ratio, Bus-Ratio, and Bike-Ratio. The spatial distribution of these four ratios is shown in Figure 4. Figure 4(a) shows that the Car-Ratio is lower in the townships in Guangzhou, Shenzhen, and Hongkong (i.e., the blue area where the Car-Ratio <0.557). In contrast, the Car-Ratio of the townships in cities with lower levels of development is higher, such as Zhaoqing, Foshan, and Jiangmen. The townships in lower levels of development cities may be relatively remote in location and have relatively less developed transportation networks. Lacking convenient public transport and transport facilities, residents prefer to drive as their main mode of transport, resulting in a higher Car-Ratio.

In contrast, the results of the other three transport modes (i.e., Subway-Ratio, Bus-Ratio, and Bike-Ratio) in Figures 4(b)-(d) are different from that of Car-Ratio. In particular, the cold spots and hot spots in Subway-Ratio are almost opposite to Car-Ratio. In Guangzhou, Shenzhen, and Hong Kong, which have a high level of development, the Subway-Ratio is the highest, while in contrast, Zhaoqing, Foshan, and Jiangmen, which have a low level of development, have the lowest values. The value of Bus-Ratio is high in the townships in the center of Guangzhou and in Hong Kong, the townships in Zhaoqing, which is different from the distribution of other

modes. It is worth noting that since the values of the Bike-Ratio itself are relatively small, the difference between the townships, although different in color, is not large. The areas with high bike ratios are concentrated in the center of Guangzhou, which is the largest red area in the middle of the figure.

However, in other studies of GBA's transportation CO_2 emissions, the results show that the central cities for economic development, Guangzhou, Foshan, Dongguan, Hong Kong, and Shenzhen have relatively high CO_2 emissions (Wang et al., 2023). The conclusions of this study are different from the above, on the one hand, because the "Ratio" selected is a relative value, so the large CO_2 emissions ratio does not mean the large emissions. On the other hand, this study selects the emissions from four modes of intra-city transport, which are different from the total emissions from the whole transport system of freight and passenger transport.

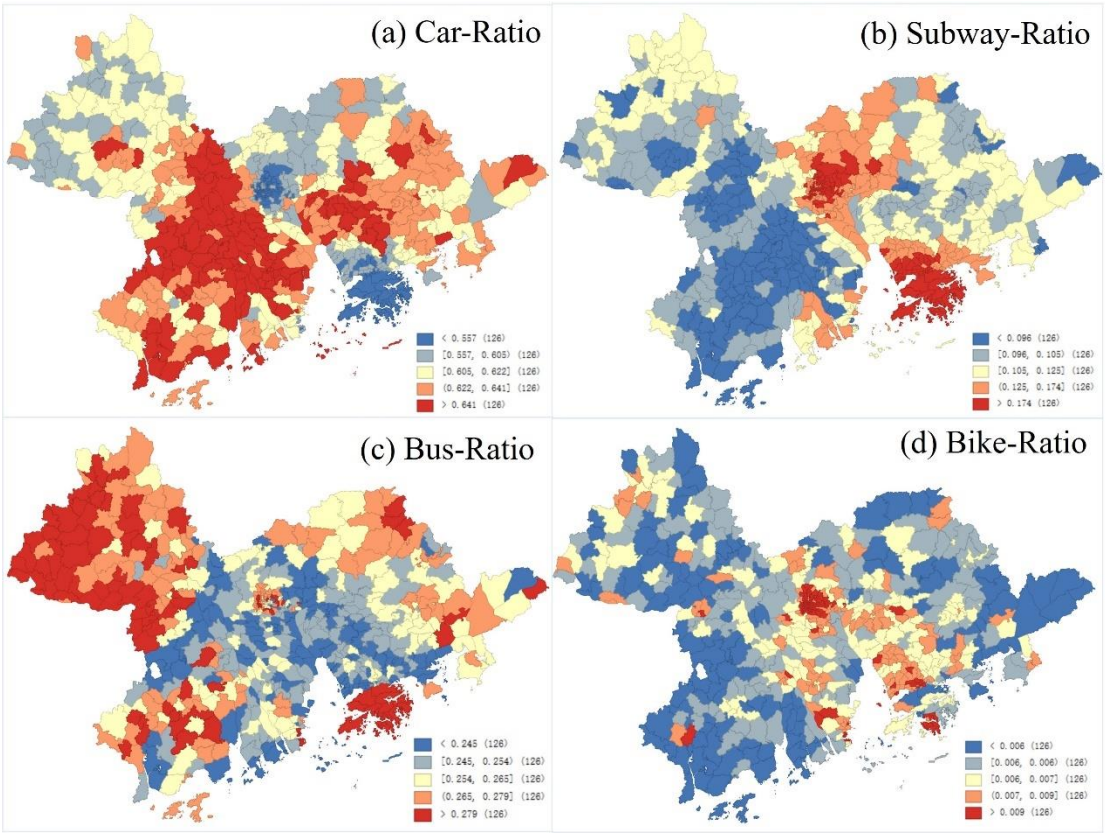

Figure 4. Spatial distribution of ratios of CO_2 emission from the four transport modes

The global Moran's I of CO_2 emission ratios of each transport mode is shown in

Figure 5. The Z-score for all Moran's I meet the significance threshold ($p < 0.001$), as shown in Table 4. In detail, Moran's I indices for four ratios Car-Ratio, Subway-Ratio, Bus-Ratio, and Bike-Ratio are 0.883, 0.886, 0.706, and 0.776, respectively. The results suggest that the CO_2 emissions ratio from each transport mode is highly positively correlated at the township level. In the scatterplots, the majority of points are concentrated in the first and third quadrants, affirming the presence of spatial positive autocorrelation in most townships. In these subfigures of Figure 5, there is a special agglomeration region (i.e., Zone a) in the third quadrant of the Car-Ratio, which is dispersed from most of the other points. These townships in the "Zone a" of Car-Ratio are all located in Hong Kong, suggesting that there is a very obvious negative spatial correlation in the Car-Ratio between these townships in Hong Kong compared with other townships.

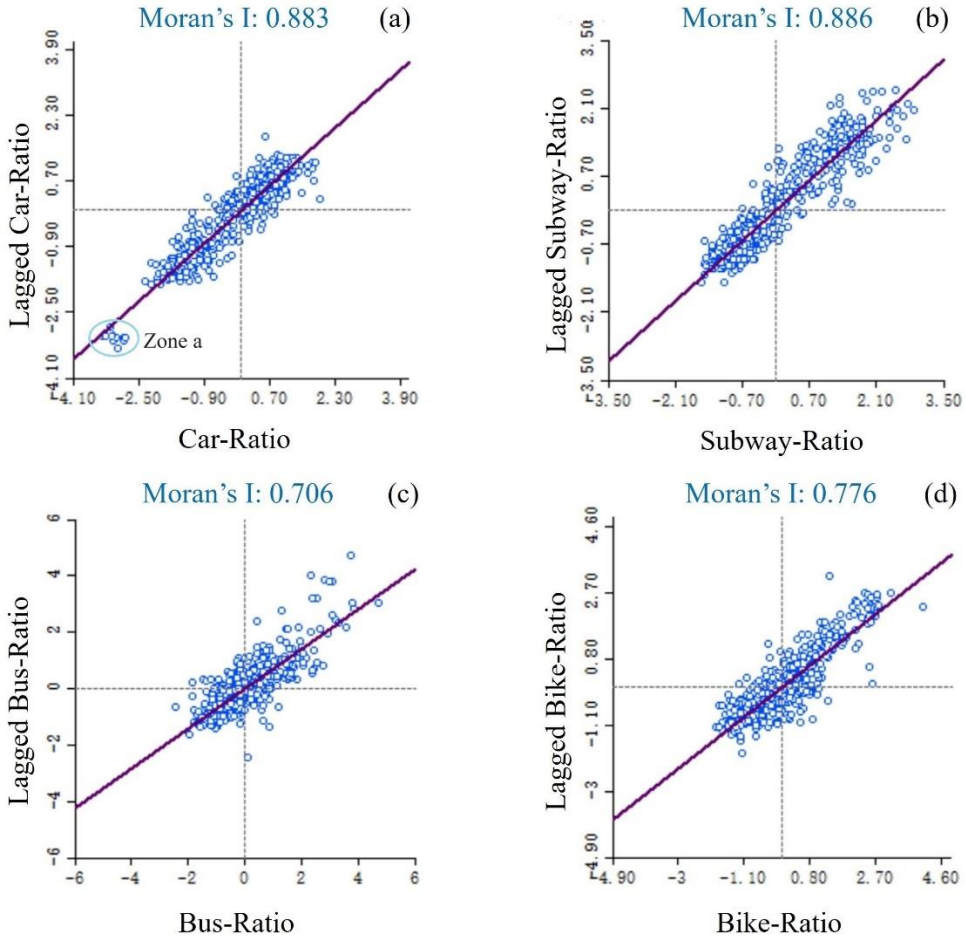

Figure 5. Global Moran's I of CO_2 emissions ratios of four transport modes

546 Table 4. Global Moran's I of ratios between two modes

Type	Moran's I	P-value	Z-value
Car-Ratio	0.883	0.000	28.313
Subway-Ratio	0.886	0.000	28.204
Bus-Ratio	0.706	0.000	23.419
Bike-Ratio	0.776	0.000	24.963

547 To elucidate the spatial local clustering characteristics of the four ratios, Figure 6
548 presents the local LISA clustering map. The four quadrants of the Moran scatterplot
549 correspond to four cluster types: high-high cluster (H–H), high-low cluster (H-L), low-
550 high cluster (L-H), and low-low cluster (L-L). In detail, H–H denotes that the township
551 exhibits a spatial positive correlation with adjacent townships having high values,
552 indicating a pronounced spatial dependence. L–L denotes the spatial positive
553 correlation for low values. In addition, H-L implies that townships display a spatial
554 negative correlation with adjacent townships having low values, signifying significant
555 spatial heterogeneity, and L-H denotes a similar negative correlation. In the four
556 subfigures, more townships have H–H and L-L agglomeration types, confirming the
557 conclusion that the CO_2 ratio in the GBA has positive spatial autocorrelation at the
558 township level. On the whole, Car-Ratio shows spatially that H-H townships are
559 dominant, Subway-Ratio features a predominance of L-L townships, Bus-Ratio shows
560 about the same number of H-H townships as L-L, and Bike-Ratio presents the largest
561 number of L-L townships. In addition, as shown in Figure 6(a) and Figure 6(b), the H-
562 H and L-L clustered townships in Car-Ratio are essentially opposite in Subway-Ratio.
563 Especially, Car-Ratio presents H-H in the townships of Guangzhou city center and
564 Shenzhen Hong Kong, respectively, but Subway-Ratio in the townships of these two
565 regions presents the opposite L-L. Comparing Figure 6(b) and Figure 6(d) reveals that
566 there is a significant overlap between the H-H and L-L townships of Subway-Ratio and
567 Bike-Ratio.

568 Overall, the distribution of Car-Ratio is significantly different from the other three
569 ratios, in the townships where this ratio presents H-H, while the other three ratios are
570 predominantly L-L distributed. In addition, especially in the two areas where the Car-
571 Ratio presents L-L (blue areas in Figure 6(a)), the corresponding Subway-Ratio
572 presents H-H, the corresponding Bus-Ratio in the lower-right blue areas in Figure 6(a)
573 also presents H-H, and a small number of townships in the two blue areas in Figure 6(a)

Bike-Ratio show H-H. Areas with high Car-Ratio and low use of other transport modes may lack efficient public transport infrastructure. Conversely, areas with high public transport usage may have robust metro and bus networks. In addition, these results may be related to the competitive or cooperative relationship between the various transport modes, and these will be revealed below based on the bivariate Moran's I. For example, the Bus-Ratio insignificance in the H-H clustering areas in Car-Ratio might stem from the relatively weak competition between buses and cars in these townships, which will be analyzed further below based on quantitative results.

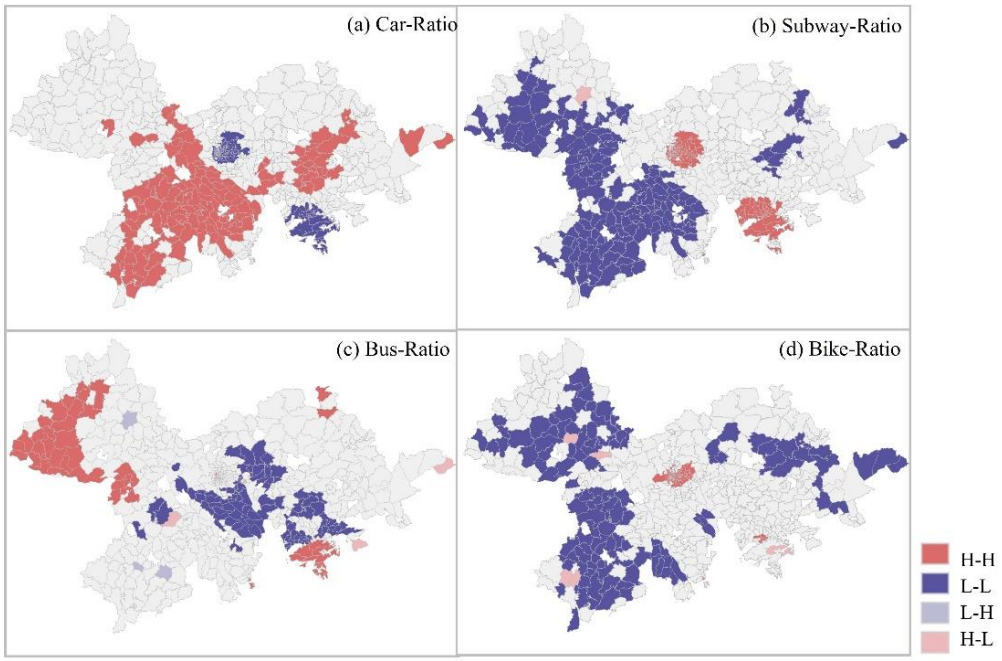

Figure 6. LISA for CO_2 emissions ratios of four transport modes

4.2 Spatial autocorrelation of bivariate modes for CO_2 emission ratios

As described in **Section 3.3**, this study calculates Moran's I index for two-by-two groups of the four transport modes, and the values shown in Table 5. Scatterplots of the 12 bivariate Moran's I are displayed in **Appendix A**. These results show that Car-Ratio is spatially negatively correlated with Subway-Ratio, Bus-Ratio, and Bike-Ratio, with Moran's I indices of -0.798 ($p<0.001$), -0.351 ($p<0.001$), and -0.574 ($p<0.001$). Among them, Car-Ratio and Bus-Ratio have the lowest negative spatial correlation, which supports the weak competitive relationship between these two transport modes

proposed above. It is worth noting that Subway-Ratio and Bus-Ratio are positively correlated but the degree of correlation is very low, i.e., the Moran's I index is 0.006. In addition, Subway-Ratio and Bike-Ratio have a high spatial correlation, with a Moran's I index of 0.570 ($p<0.001$). Bus-Ratio and Bike-Ratio have a low spatial correlation with a Moran's I index of 0.101 ($p<0.001$).

Table 5. Global bivariate Moran's I of ratios of two transport modes

Moran's I	Car-Ratio	Subway-Ratio	Bus-Ratio	Bike-Ratio
Car-Ratio	0.883***	-0.798***	-0.351***	-0.574***
Subway-Ratio	-0.792***	0.886***	0.006	0.570***
Bus-Ratio	-0.361***	0.018	0.706***	0.101***
Bike-Ratio	-0.581***	0.577***	0.103***	0.776***

Note: ***, **, * indicate significance at the 0.99, 0.95, and 0.90 confidence levels, respectively.

As shown in Table 5, the values of the two variables interchanging their positions in the bivariate Moran's I are similar. Hence, 6 group variables are selected to show the spatial agglomeration, as shown in Figure 7. Specifically, Figure 7(a) is dominated by H-L and L-H i.e., mainly spatially negative correlations. The largest number of townships presenting H-L are mainly located in the left half of the figure in cities with a low level of development, i.e., in these townships the value of the Car-Ratio itself is high and the value of the Subway-Ratio of the adjacent townships is low. In addition, the L-H townships are located in Guangzhou, Shenzhen, and Hong Kong, which have higher levels of development. Figure 7(d) shows that Subway-Ratio and Bus-Ratio in townships located in the Hong Kong area show H-H, which is the largest red area in the figure. The urban planning structure in Hong Kong may contribute to a positive correlation in CO_2 emissions Ratios between the subway and bus. The subway and bus routes overlap in certain areas, leading to high-frequency services in those regions, which could result in increased CO_2 emissions for both subway and bus in those specific areas. There is a distinct red area in Figure 7(e) located in the center of the city of Guangzhou. Subway-Ratio and Bike-Ratio show a positive correlation (i.e., H-H) in this area. This may be related to the information that Guangzhou is a passenger transport

system with rail as the backbone and that passengers in the city center may use the subway for major long-distance trips, but may be more inclined to use bikes for the last short distance (the last kilometer) (Lv et., 2021).

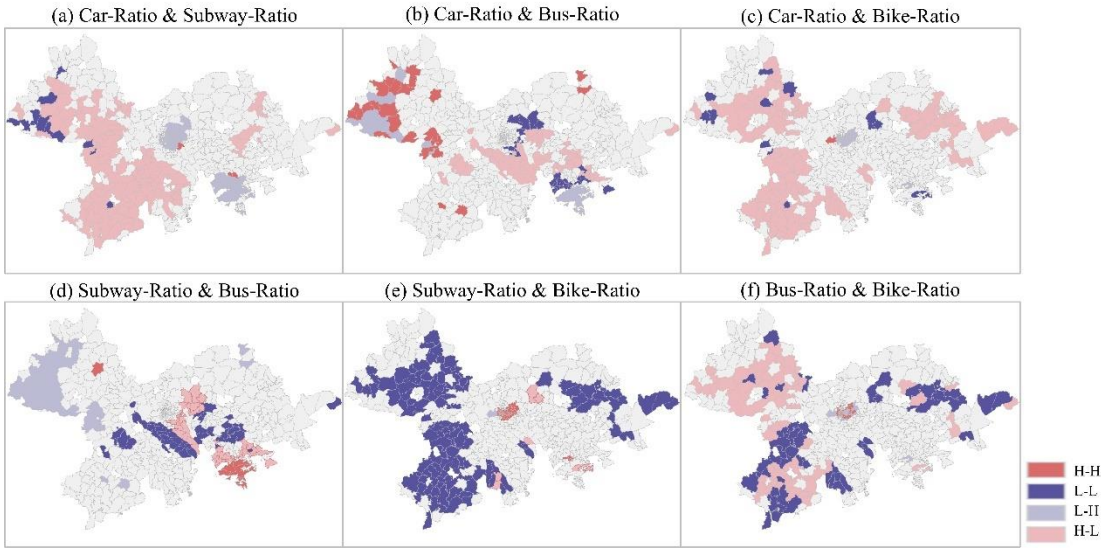

Figure 7. LISA for ratios of transport modes based on bivariate Moran's I index

4.3 Influencing factors of CO_2 emission ratios

In this subsection, SEM is employed to explore the impact of factors on the CO_2 emission ratios of different transport modes. As described in subsection 3.4, the selection of SEM is based on the LM test and the LR test, which is shown in Table 6. Specifically, combining the third and fourth rows in the table, robust LM-Lag tests accept the hypothesis that the explained variables do not exist in spatial autocorrelation, so the spatial lag model (SLM) is not applicable. As shown in the fifth and sixth rows of the table, LM-Error and robust LM-Error tests reject the hypothesis that random errors do not have spatial autocorrelation, so the SEM should be used. Therefore, SEM is chosen in this study to explore the influencing factors of four CO_2 emission ratios. Table 6 displays the regression outcomes of the SEM, with the R^2 values for the four SEM models being 0.791, 0.817, 0.593, and 0.734, respectively. The "Lambda" represents the spatial lag coefficient for each ratio, which measures the strength of

spatial correlation. A larger "Lambda" indicates that the CO_2 emission ratios of different transport modes are strongly influenced by the surrounding spatial units (i.e., townships). In all modes, "Lambda" values are highly significant, indicating a significant spatial correlation in the CO_2 emission ratios of transportation. The explanation of the coefficients in models is detailed as follows.

Table 6. Explanatory variables of four ratios

	Car-Ratio	Subway-Ratio	Bus-Ratio	Bike-Ratio
Moran 'I (error)	0.546	0.588	0.408	0.336
LM-lag	11.2108***	168.9346***	42.63311***	78.9342***
Robust LM-lag	0.079	5.1338*	14.3018***	16.6434***
LM-error	358.9528***	416.7026***	200.2015***	135.8577***
Robust LM-error	347.8214***	252.9018***	171.8721***	73.5670***
R^2	0.791	0.817	0.593	0.734
CONSTANT	0.616	0.126	0.255	0.007
Residence	0.008*	-0.002	-0.004	-0.001***
Mall	0.037	-0.049	0.011	-0.004**
Hotel	-0.011	-0.002	0.014*	0.001**
Factory	0.087**	-0.125***	0.030	0.001
Bus station	-0.193***	0.064**	0.141***	0.008***
School	0.036**	-0.032**	-0.005	0.001
Office building	-0.009	0.019	-0.010	-0.001
Restaurant	-0.007	0.003	0.005	0.001**
Subway station	0.107	0.250	-0.389	-0.052***
POP	-0.290***	0.229***	0.028	0.025***
Trunk	1.261	-1.001	-0.494	-0.042
Tertiary	1.813	1.029	-3.295***	-0.110*
Secondary	-2.377*	3.092***	-1.052	0.168***
Primary	1.732	-0.945	-0.548	0.010
Motorway	-0.336	-1.932	2.418*	-0.130
Center-distance	0.000***	0.000***	0.000	0.000***
Land use diversity	-0.024***	0.014**	0.005	0.001*
Lambda	0.783***	0.818***	0.653***	0.671***

Note: ***, **, * indicate significance at the 0.99, 0.95, and 0.90 confidence levels, respectively.

According to Table 6, it is possible to obtain the important factors that have an impact on the CO_2 emission ratio and to explain the heterogeneous effect of the same factor on the emission ratio of different transport modes. The three factors of “POP”, “Secondary”, and “Land use diversity” have significant negative effects on Car-Ratio, significant positive effects on Subway-Ratio and Bike-Ratio, and insignificant effects on Bus-Ratio. Similarly, Wang et al (2023) found that the population and economic variables have higher facilitation to the growth of CO_2 emissions in GBA. At the same time, these factors affect Subway-Ratio to a greater extent than Bike-Ratio. In detail, the coefficient of population density (POP) is negative in the model of Car-Ratio, and it passes the significance test of 0.05. This shows that population agglomeration has an adverse impact on Car-Ratio. Densely populated areas usually indicate more traffic demand and congestion problems, resulting in low car usage, and in turn reduces the proportion of CO_2 emission induced by cars (i.e., Car-Ratio). The coefficient of 0.229 for “POP” in the “Subway-Ratio” model indicates a statistically significant positive relationship between population density and the CO_2 emission ratio of subway usage. The increase in population density may lead to traffic congestion and further promote subway usage as a quicker and larger volume of travel option compared to other modes of transportation, leading to additional CO_2 emissions from subways. In addition, the coefficient of “POP” for the “Bus-Ratio” and "Bike-Ratio" are 0.028 and 0.025 ($p<0.01$), indicating the influence of population density on Bus-Ratio and Bike-Ratio is not great. The coefficient of “Secondary” in models of Car-Ratio and Subway-Ratio are -2.377 and 3.092 respectively. As the length of secondary roads increases, the CO_2 ratio of cars decreases, possibly reflecting the fact that longer roads may prompt greater use of public transportation options, such as the subway, to reduce the use of personal automobiles. In the result of the Car-Ratio model, the influence coefficient of land use diversity is -0.024. This result suggests that an increase in land use diversity has a negative impact on Car-Ratio. It may be that the increase in land use diversity means that there are more types of land within the township, including commercial areas,

residential areas, parks, and green spaces. This diversity may encourage the adoption of sustainable transport modes, such as walking, cycling, and public transport, thereby reducing the need for and use of cars, which in turn reduces CO_2 emissions.

Unlike the results of SEM, which assigns single coefficients to each variable, SHAP provides a more nuanced analysis by capturing non-linear relationships between variables and emission ratios. It also accounts for interactions between variables, offering a deeper understanding of how these factors combine to influence outcomes. Additionally, SHAP can detect specific thresholds where variables significantly change their impact, revealing insights that may be missed by SEM's linear coefficients. Specifically, Figure 8 shows the SHAP value distribution of the explanatory variables, with each dot representing the value of a township in GBA. Each dot is colored according to the variable's value in a particular township, with blue representing a lower value and red representing a higher value. If the variable is associated with a decrement in the estimated income, the dot will be shown on the left side of the figure, indicating that the variable has a negative SHAP value (and vice versa). The heterogeneity of the effects of the same variable on different ratios can be seen in Figure 8 in two ways. One is the difference in the ordering of importance. For example, the order of the variable "Centre-distance" in the four subfigures is 3rd, 4th, 6th, and 6th respectively. The other is that although the same variable has the same ordering in the plots of the four ratios, the trend of the impact is different. In detail, the SEM residuals are ranked first in all four subfigures, but their scatter distributions have different trends. Moreover, Figure 9 shows the specific effect of Centre-distance on the four ratios. As can be seen from the figure, these subfigures have different trends, and the corresponding threshold effects will be different. Specifically, in Figure 9(a) as the value of the horizontal coordinate increases, its effect on Car-Ratio first increases and then levels off. This corresponds to a trend change threshold of approximately 50. Similarly, the thresholds in Figures 9(b)-(d) are about 60, 40, 60 respectively. These findings can provide some basis for differentiated policy development for different travel modes in a low-carbon context.

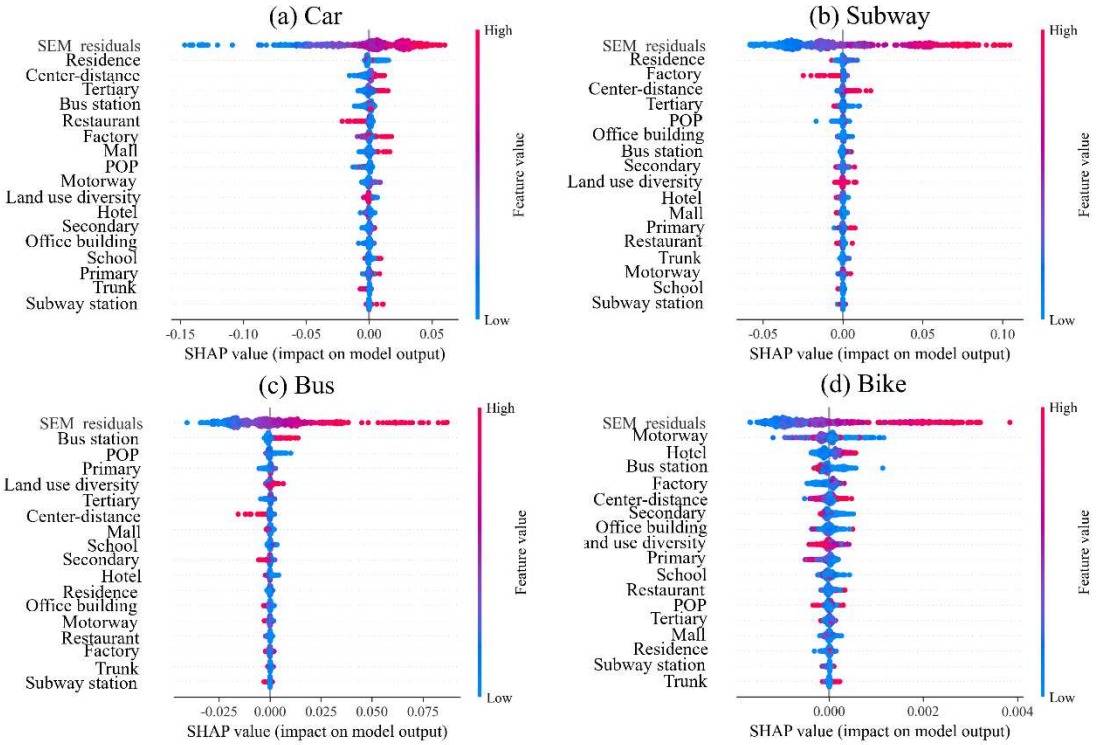

Figure 8 The SHAP value indicating the contribution of individual explanatory variables to four ratios

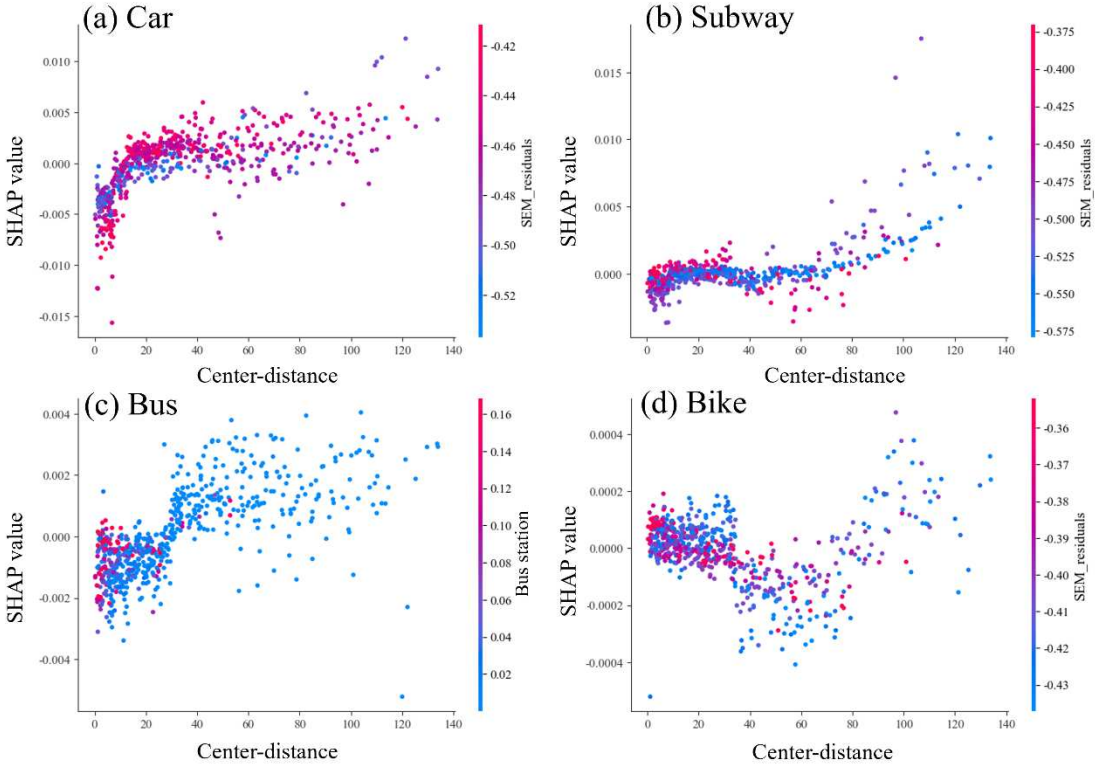

Figure 9 Scatterplot of the effect of Centre-distance on four ratios

4.4 Spatial autocorrelation of CO_2 emission at different spatial scales

By integrating the township-level data, Moran's I index of the four ratios at the district level and the city level is further calculated, as detailed in Table 7. The results show that Moran's I index of the four ratios at different scales changes considerably. From township to district to city, the significance of Moran's I index becomes less and less. Moreover, the positive and negative values of Moran's I index change due to the change in spatial scale. For example, Bus-Ratio and Bike ratio become negatively correlated at the city level scale. Additionally, Moran's I index for Car-Ratio and Subway-Ratio at the city level is 0.218 and 0.330, respectively. These values are similar to the findings of Wang et al. (2023), which reported that the transport emission Moran's I index for 11 cities in the GBA fluctuates between 0.27 and 0.3.

Figure 10 illustrates the global Moran's I scatterplots at the district level. By comparing the results in Figure 6 at the township level, Moran's I index for all four ratios becomes smaller after aggregating the township into the district scale. In particular, Moran's I index corresponding to Bus-Ratio changes from 0.706 ($p<0.01$) to 0.220 ($p<0.1$). Specifically, the spatial clustering of each ratio at the district level is demonstrated in Figure 11. Comparing the spatial clustering maps in Figure 6 at the township level and in Figure 11 at the district level, the results show that the main H-H, H-L, L-H, and L-L areas remain unchanged after the spatial scale of the study is expanded, but many details are lost.

Table 7. Global Moran's I of ratios at different spatial scales

Type	Township Level	District Level	City Level
Car-Raio	0.883***	0.659***	0.218
Subway-Raio	0.886***	0.776***	0.330
Bus-Raio	0.706***	0.220*	-0.200
Bike-Raio	0.776***	0.529***	-0.267

733

734 Note: ***, **, * indicate significance at the 0.99, 0.95, and 0.90 confidence levels, respectively.

735

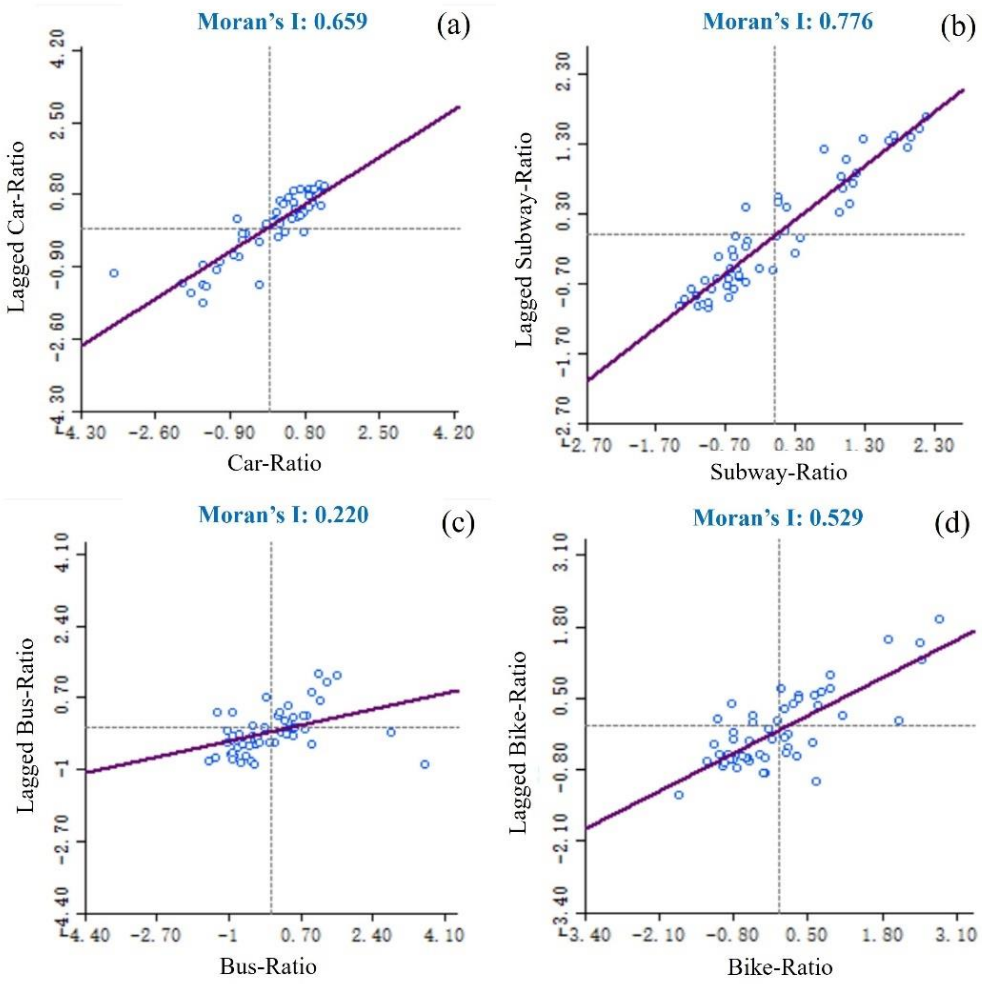

736

737 Figure 10. Global Moran's I scatterplots at the district level

738

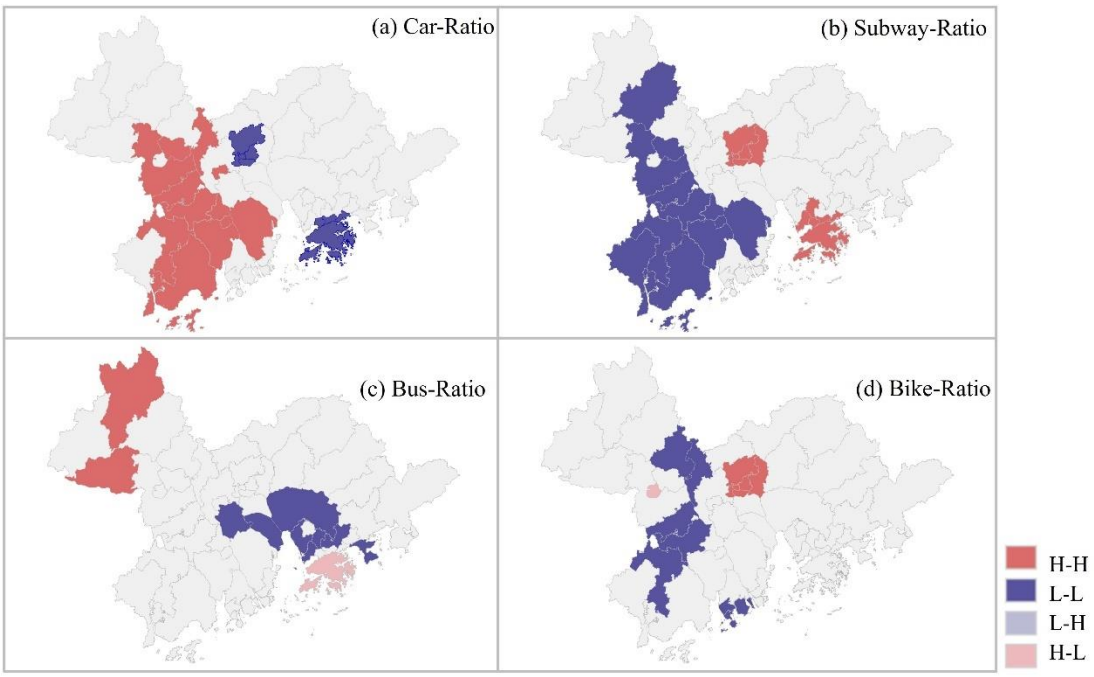

Figure 11. LISA at the district level

There may be several reasons why Moran's Index of the ratio of CO_2 from the four transport modes is most significant at the township level. First, there may be significant spatial differences in the distribution of transport modes across townships, e.g., downtown areas may prefer subways and buses, while suburban areas may prefer driving and cycling. Such differences in spatial distribution can lead to increased spatial correlation in the ratio of transport modes. Second, each township may have different characteristics in terms of transport facilities, road networks, and population density, and these factors can have an impact on the choice and share of different transport modes. In contrast, district and city-level data integrate a larger area where regional characteristics may be more evenly distributed, resulting in a weaker spatial correlation of transport mode shares. Third, there may be a degree of averaging and blending effects when data are aggregated from the township level to the district or city level, leading to a weakening of the spatial relevance of the transport mode share. Fourth, studies at the township level are closer to the local scale, and the smaller spatial scale allows for more consistency and correlation in the transport mode share. On the other hand, studies at the district and city levels are closer to the overall scale, covering a larger spatial area,

and may have more spatial variability and heterogeneity. This results in a weaker spatial correlation of CO_2 emissions ratios of four transport modes.

In addition, it is worth noting that the spatial autocorrelation of the emission ratios of the four transport modes varies to different extents at different spatial scales. As the spatial scales converged from township level to district level, the smallest change was Subway-Ratio (from 0.886*** to 0.776***) and the largest change was Bus-Ratio (from 0.706*** to 0.220*). When spatial scales converge from township level to city level, the smallest change is still in Subway-Ratio (from 0.886*** to 0.330), and the largest change is in Bike-Ratio (from 0.776*** to -0.267). The relatively stable spatial autocorrelation of the subways at different spatial scales may be related to their long-distance traveling tasks in the urban transport network. The subway system usually connects different areas of a city and provides fast and efficient transport services, which are suitable for long-distance commuting and inter-regional traveling. On the contrary, the spatial autocorrelation of bikes is relatively unstable at different spatial scales, probably because bikes mainly undertake short-distance traveling tasks. Bikes are usually used to solve the last-mile problem in cities, i.e., the demand for short-distance travel from public transport stations to destinations. As cycling trips are affected by factors such as terrain, road conditions, and parking facilities, the distribution of cycling use is more dispersed and diversified, resulting in relatively unstable spatial correlations at different spatial scales.

5. Discussions

A spatial perspective study on CO_2 emissions from various modes at the fine-grained street level within urban agglomerations has not existed before. Unlike previous studies that predominantly focused on the transportation sector as a whole or on individual modes, our study focuses on the CO_2 emission from cars, subways, buses, and bikes at the township level and explores multiple modes' patterns and influencing factors from a spatial perspective, thereby addressing a critical gap in the literature. In

detail, the innovations of this study are primarily reflected in the following aspects. (a) Comparative spatial analysis of multiple transport modes: Unlike previous studies that have primarily focused on quantitative comparisons of carbon emissions, this research offers a novel perspective by conducting a comparative analysis of the spatial distribution of CO_2 emissions across different transportation modes within the same region. (b) Fine-scale analysis in urban agglomerations: This study is pioneering in its examination of transportation-related carbon emissions at a fine-grained level, such as the street scale, within a large urban agglomeration. Previous research has not explored carbon emissions at such a detailed spatial scale across a wide city cluster. (c) Integration of Spatial econometric and machine learning models: The study introduces a unique methodological framework that combines spatial econometric models with machine learning models. This integration allows for the simultaneous exploration of spatial relationships and nonlinear interactions, offering a more comprehensive understanding of the factors influencing carbon emissions in urban transport systems.

6. Policy implications

The findings of this study can provide some policy insights for local and international practices to promote CO_2 emission reduction and achieve carbon emissions peaking at an early date.

Firstly, in terms of the spatial distribution of the emission ratio for the single transport mode, it can be seen that the spatial pattern of the CO_2 emission ratio varies for each transport mode. The average value of the ratio of CO_2 emissions from car travel (i.e., Car-Ratio) in the total CO_2 emissions generated by the four transport modes is 0.60. Meanwhile, the LISA plot shows the townships where Car-Ratio shows an H-H clustering, which should be a key area of focus for government administrators. It should be noted that townships with H-H clustering in Car-Ratio are likely to have total transport carbon emissions that are not very high. By comparing Figure 6(a) with C-1 in Appendix C, townships with high Car-Ratio and total carbon emissions are the

812 primary targets for reducing transport carbon emissions, which can be set up as the
813 "Carbon Reduction Pilot Zone" in the GBA. Therefore, the important step is to reduce
814 the CO_2 emissions from car trips in these Zones by reducing the cars' own emissions or
815 increasing the use of other modes. On the one hand, regulators can provide new energy
816 subsidies to change the power type of cars to reduce CO_2 emissions in the "Carbon
817 Reduction Pilot Zone". On the other hand, low carbon travel incentives or car
818 congestion pricing could then be implemented in the "Carbon Reduction Pilot Zone" to
819 promote a shift in car travelers to lower carbon transport modes (e.g., subways, buses,
820 and bikes).

821 Secondly, from Moran's I index and LISA plots of CO_2 emission ratios for multiple
822 pairs of transport modes, there is a positive spatial correlation between any two of the
823 three modes (i.e., subway and bus and bike) in the GBA. This result spatially illustrates
824 that subway, bus, and bike are not exactly in competition, but are generally seen to be
825 in a combined relationship. This discovery can provide a basis for the implementation
826 of Mobility as a Service (MaaS) systems in the GBA areas. The core idea of MaaS is to
827 integrate various transport modes (such as public transportation, taxis, bike-sharing,
828 walking, etc.) into a single platform to provide user-customized travel planning,
829 booking, payment, and information inquiry services through an app, which helps reduce
830 private car use. It has been shown that MaaS could shift users' mobility behavior toward
831 more sustainable transport modes (i.e., from private and low-capacity modes to public
832 transport) (Hasselwander et al., 2022). Managers can integrate more modes of
833 transportation in areas where multi-modal integration is already occurring to increase
834 the efficient use of public transportation to replace more private vehicle trips and
835 enhance connectivity between modes of transportation in areas where modal integration
836 is not yet occurring. Moreover, the findings suggest that population density, road length,
837 and land use diversity are the key drivers of CO_2 emission ratios, and the same factor
838 has different directions and degrees of influence on the emission ratios of different
839 modes. For example, land use diversity has significant negative influences on Car-Ratio,

significant positive influences on Subway-Ratio and Bike-Ratio, and insignificant influences on Bus-Ratio. Encouraging diverse land use patterns can be effective in reducing the proportion of car emissions while increasing the proportion of subway and cycling. Governments should prioritize zoning policies that favor mixed-use, integrating residential, commercial, and recreational spaces within communities. Such an approach not only reduces reliance on cars but also promotes active modes of transport like cycling and walking, contributing to sustainable urban mobility.

Thirdly, urban planning and transportation policies should be tailored to specific local contexts. In this study that focuses on the emission of cars, subway, buses, and bikes, the findings at the township level reveal that different townships exhibit similar trends in transport mode choices, suggesting that targeted and focused approaches can be employed to address transport emissions at smaller spatial scales. However, as data is aggregated to larger administrative levels such as districts and cities, the influence of spatial heterogeneity becomes more prominent, necessitating more flexible strategies to accommodate diverse regional needs. Urban agglomerations involve many cities and administrative regions, and the management of CO_2 from transport modes requires cross-boundary cooperation, enhanced information sharing, and policy coordination. In addition, results demonstrate that the spatial correlation of CO_2 from different transport modes varies across different spatial scales. Among the four transport modes, the spatial autocorrelation of Subway-Ratio is relatively stable across scales, while the spatial autocorrelation of Bike-Ratio is the least stable. Therefore, when conducting transport emission studies, careful consideration should be given to the choice of spatial scale, as it can affect the interpretation of results and the formulation of policy recommendations.

Finally, the findings based on GBA offer the following policy insights for other countries. (a) The study highlights the importance of balancing private vehicles with public transit. Other countries can learn from this by enhancing the appeal and coverage of public transportation to reduce private car use and lower carbon emissions. (b) The GBA study demonstrates the value of coordinated regional planning. By adopting

unified policy frameworks and coordinated transportation planning, cities can achieve more efficient resource allocation and better carbon emission management. This approach can serve as a reference for other countries with similar urban clusters. (c) The study suggests that a detailed analysis of various transportation modes and their carbon emissions can lead to more targeted policies. For example, stricter emission standards or greater financial support in high-emission areas may effectively control and reduce traffic-related carbon emissions. Other countries can develop similar fine-tuned policies based on their specific circumstances.

7. **Conclusions**

Unlike previous studies that focused on CO_2 emissions from an individual transport mode or the whole transport system, our study focuses on multiple transport modes to explore the environmental dimension of sustainable transport systems from a spatial perspective, which is based on the CO_2 emission of 630 townships in the GBA. Specifically, we reveal the spatial clustering or dispersion of CO_2 ratios from different transport modes by applying the univariate Moran's I index. In addition, we reveal the spatial interactions and correlations between different transport modes using the bivariate Moran's I index. Furthermore, we applied SEM to explore the effects of various factors on different CO_2 emission ratios, which can consider spatial dependence and spatially lagged variables. Through SEM modeling, we uncover the factors influencing the transport of CO_2 emissions and understand their spatial mechanisms. Subsequently, the interpretable machine learning models are used to further reveal the nonlinear relationships. In addition, we expand the scale of the study to examine the spatial correlation of transport CO_2 emissions at districts and city levels. The results show that. Moran's I indices for Car-Ratio, Subway-Ratio, Bus-Ratio, and Bike-Ratio are 0.883, 0.886, 0.706, and 0.776 respectively. In addition, the results demonstrated spatial interdependencies and correlations between different transport modes, especially the subway and car with a Moran's I index of -0.798 and the subway and bike

with 0.570. This is one of the key findings of our study and the spatial relationship between CO_2 emissions from different modes has not been quantified in previous literature. The R^2 of SEM for the CO_2 ratios of the four transport modes is 0.791, 0.817, 0.593, and 0.734 respectively. Population density, Primary, and Land use diversity are among the key drivers, and population agglomeration has an adverse impact on Car-Ratio. The results of interpreterable machine learning models show that even when a variable maintains the same order of importance in the subfigures, its effect on the CO_2 emission ratios can show different trends. In addition, the results showed variations in spatial patterns and heterogeneity of CO_2 across different geographic scales, which can complement the findings of previous studies based on the single geographic scale. These insights can inform urban planners, policymakers, and transportation authorities in developing targeted strategies to reduce CO_2 and foster more sustainable and environmentally friendly transportation systems.

While our study made an understanding of the spatial characteristics and influencing factors of CO_2 from multiple transport modes, several limitations should be acknowledged. Our study primarily focused on the spatial aspects of CO_2 from transportation. However, the temporal dynamics, such as daily and seasonal variations, were not explicitly considered in this analysis due to a lack of data. Incorporating temporal variations and trends could provide a more comprehensive understanding of CO_2 dynamics and inform time-sensitive policy interventions. In addition, our study focuses on the environmental dimension of sustainable transportation based mainly on CO_2 emissions and lacks further exploration of the social and economic dimensions. In the future, the social dimensions of sustainable transportation in terms of accessibility to employment, spatial equity, community cohesion, safety, transportation variety, etc., can be explored based on obtaining relevant data. Regarding the economic dimension of sustainable transport, it is necessary to further obtain the relevant data on travel time, travel cost, and indirect transportation cost for users, etc., for research in the future. Moreover, this study finds that the spatial autocorrelation of the emission ratios of

different transport modes (i.e., car, subway, bus, and bike) at different scales varies tremendously, which can be further explored in the future by combining the actual traveling information of the residents, especially the traveling distance and traveling frequency.

Acknowledgments

This project is supported by the National Natural Science Foundation of China (No. 20221300672) and Carbon Neutrality and Energy System Transformation (CNEST) Program led by Tsinghua University. The authors thank the anonymous reviewers for their comments and suggestions that helped improve the manuscript.

Appendix A. Global bivariate Moran's I scatterplots of bivariate modes

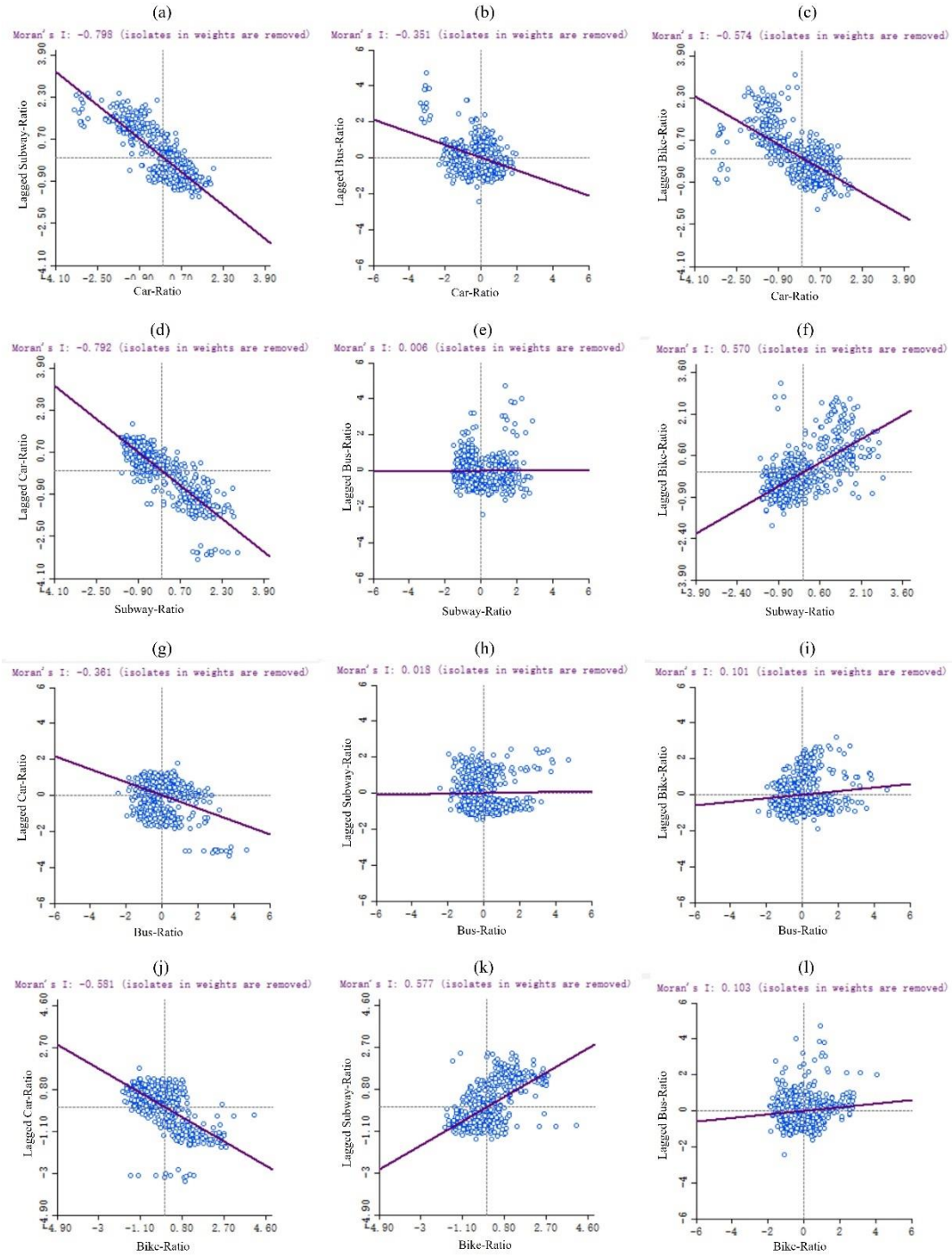

Figure A-1. Global bivariate Moran's I scatterplots of CO_2 emission ratios

Appendix B. VIF result of all explanatory variables

Table B-1 VIF result of explanatory variables in SEM

Variables	VIF
Residence	5.319
Mall	3.883
Hotel	3.282
Factory	1.400
Bus station	5.095
School	2.155
Office building	6.453
Restaurant	8.573
Subway station	6.469
POP	2.234
Trunk	4.612
Tertiary	2.505
Secondary	2.421
Primary	5.046
Motorway	1.439
Center-distance	1.580
Land use diversity	1.416

Appendix C Spatial distribution of total CO_2 emissions of four modes

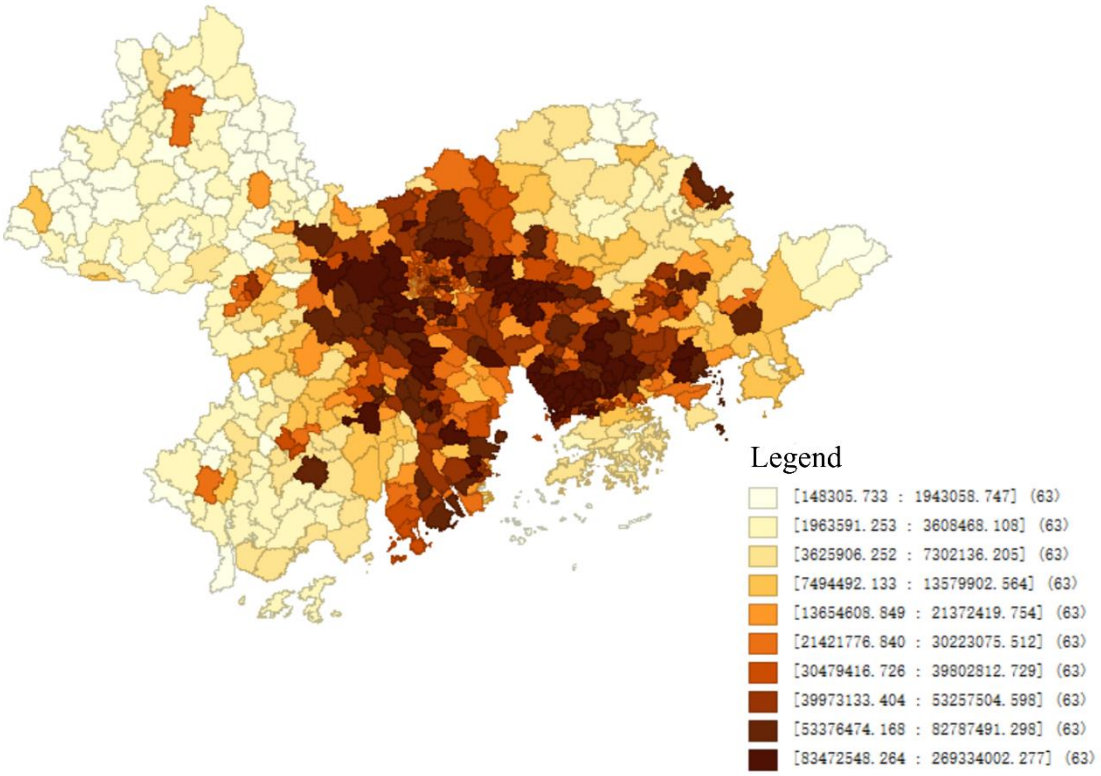

Figure C-1 Spatial distribution of total CO_2 emissions of four modes (unit: kg)

References

1. Allen M, Dube O, Solecki W, et al. Global warming of 1.5 C. An IPCC Special Report on the impacts of global warming of 1.5 C above pre-industrial levels and related global greenhouse gas emission pathways, in the context of strengthening the global response to the threat of climate change, sustainable development, and efforts to eradicate poverty. *Sustainable Development, Efforts to Eradicate Poverty.* 2018.
2. An R, Wu Z, Tong Z, Qin S, Zhu Y, Liu Y. How the built environment promotes public transportation in Wuhan: A multiscale geographically weighted regression analysis. *Travel Behaviour and Society.* 2022;29:186-199.
3. Anselin L. Local indicators of spatial association—LISA. *Geographical analysis.* 1995;27(2):93-115.
4. Aturinde A, Farnaghi M, Pilesjo P, Mansourian A. Spatial analysis of HIV-TB co-clustering in Uganda. *Bmc Infectious Diseases.* 2019;19.
5. Basbas S, Politis I. Urban road pricing and sustainable transportation systems: The Thessaloniki central area case. *J International Journal of Sustainable Development Planning.* 2008;3(1):1-15.
6. Batur I, Bayram IS, Koc M. Impact assessment of supply-side and demand-side policies on energy consumption and CO2 emissions from urban passenger transportation: The case of

Istanbul. *Journal of Cleaner Production.* 2019;219:391-410.
7. Becker H, Balac M, Ciari F, Axhausen KW. Assessing the welfare impacts of Shared Mobility and Mobility as a Service (MaaS). *Transportation Research Part a-Policy and Practice.* 2020;131:228-243.
8. Cerrud CG, Mota IFDL, Anguiano FIS. Proposal for greenhouse gas emissions reduction in public passenger transportation - ScienceDirect. *Case Studies on Transport Policy.* 2021.
9. Chen JR, Zhou D, Zhao Y, Wu BH, Wu T. Life cycle carbon dioxide emissions of bike sharing in China: Production, operation, and recycling. *Resources Conservation and Recycling.* 2020;162.
10. Dasgupta S, Lall S, Wheeler D. Subways and CO2 emissions: A global analysis with satellite data. *Science of the Total Environment.* 2023;883.
11. Deng X, Chen W, Zhou Q, et al. Exploring spatiotemporal pattern and agglomeration of road CO2 emissions in Guangdong, China. *Science of the Total Environment.* 2023;871.
12. Deng Y, Shao S, Mittal A, et al. Incentive design and profit sharing in multi-modal transportation networks. *Transportation Research Part B-Methodological.* 2022;163:1-21.
13. Elhorst JP. *Spatial econometrics: from cross-sectional data to spatial panels.* Spatial econometrics. From cross-sectional data to spatial panels; 2014.
14. Freiria S, Sousa N, Calvo-Poyo F. Spatial analysis of the impact of transport accessibility on regional performance: A study for Europe. *Journal of Transport Geography.* 2022;102.
15. Gao K, Yang Y, Gil J, Qu X. Data-driven interpretation on interactive and nonlinear effects of the correlated built environment on shared mobility. *Journal of Transport Geography.* 2023;110.
16. Gao S, Zhang X, Chen M. Spatiotemporal dynamics and driving forces of city-level CO2 emissions in China from 2000 to 2019. *Journal of Cleaner Production.* 2022;377.
17. Gao Y, Guo C, Wei Y. Study on the dynamic evolution and synergistic relationship between urbanization and eco-efficiency through the selection of 76 agricultural counties and districts in Liaoning province as research units. *Frontiers in Ecology and Evolution.* 2022;10.
18. Garcia A, Monsalve-Serrano J, Sari RL, Tripathi S. Life cycle CO₂ footprint reduction comparison of hybrid and electric buses for bus transit networks. *Applied Energy.* 2022;308.
19. Garcia A, Monsalve-Serrano J, Sari RL, Tripathi S. Pathways to achieve future CO₂ emission reduction targets for bus transit networks. *Energy.* 2022;244.
20. Garcia-Afonso O. Impact of powertrain electrification on the overall CO2 emissions of intercity public bus transport: Tenerife Island test case. *Journal of Cleaner Production.* 2023;412.
21. Gaytan Iniestra J, Garcia Gutierrez J. Multicriteria decisions on interdependent infrastructure transportation projects using an evolutionary-based framework. *Applied Soft Computing.* 2009;9(2):512-526.
22. Girshick R, Donahue J, Darrell T, Malik J. Rich feature hierarchies for accurate object detection and semantic segmentation. Paper presented at: Proceedings of the IEEE conference on computer vision and pattern recognition2014.

23. Guimaraes VdA, Leal Junior IC. Performance assessment and evaluation method for passenger transportation: a step toward sustainability. *Journal of Cleaner Production.* 2017;142:297-307.
24. Haghshenas H, Vaziri M, Gholamialam A. Evaluation of sustainable policy in urban transportation using system dynamics and world cities data: A case study in Isfahan. *Cities.* 2015;45:104-115.
25. Han P, Lin X, Zeng N, et al. Province-level fossil fuel CO2 emission estimates for China based on seven inventories. *Journal of Cleaner Production.* 2020;277.
26. Hasselwander M, Bigotte JFF, Antunes APP, Sigua RGG. Towards sustainable transport in developing countries: Preliminary findings on the demand for mobility-as-a-service (MaaS) in Metro Manila. *Transportation Research Part a-Policy and Practice.* 2022;155:501-518.
27. He D, Liu H, He K, et al. Energy use of, and CO2 emissions from China's urban passenger transportation sector - Carbon mitigation scenarios upon the transportation mode choices. *Transportation Research Part a-Policy and Practice.* 2013;53:53-67.
28. Ibeas A, Cordera R, dell'Olio L, Coppola P, Dominguez A. Modelling transport and real-estate values interactions in urban systems. *Journal of Transport Geography.* 2012;24:370-382.
29. Joumard R, Nicolas J-P. Transport project assessment methodology within the framework of sustainable development. *Ecological Indicators.* 2010;10(2):136-142.
30. Karamanlis I, Nikiforiadis A, Botzoris G, Kokkalis A, Basbas S. Towards Sustainable Transportation: The Role of Black Spot Analysis in Improving Road Safety. *Sustainability.* 2023;15(19).
31. Kou ZY, Wang X, Chiu SF, Cai H. Quantifying greenhouse gas emissions reduction from bike share systems: a model considering real-world trips and transportation mode choice patterns. *Resources Conservation and Recycling.* 2020;153.
32. Li R, Xu M, Zhou H. Impact of high-speed rail operation on urban economic resilience: Evidence from local and spillover perspectives in China. *Cities.* 2023;141.
33. Li W, Ji Z, Dong F. Spatio-temporal evolution relationships between provincial CO2 emissions and driving factors using geographically and temporally weighted regression model. *Sustainable Cities and Society.* 2022;81.
34. Li X, Yu B. Peaking CO2 emissions for China's urban passenger transport sector. *Energy Policy.* 2019;133.
35. Li Z, Wang F, Kang T, et al. Exploring differentiated impacts of socioeconomic factors and urban forms on city-level CO2 emissions in China: Spatial heterogeneity and varying importance levels. *Sustainable Cities and Society.* 2022;84.
36. Liu C, Wang T. Identifying and mapping local contributions of carbon emissions from urban motor and metro transports: A weighted multiproxy allocating approach. *Computers Environment and Urban Systems.* 2017;64:132-143.
37. Liu J, Li J, Chen Y, et al. Multi-scale urban passenger transportation CO2 emission calculation platform for smart mobility management. *Applied Energy.* 2023;331.
38. Liu M, Jia S, He X. A quota-based GHG emissions quantification model for the construction of subway stations in China. *Journal of Cleaner Production.* 2018;198:847-

858.
39. Liu M, Jia S, Li P, Liu X, Zhang Y. Predicting GHG emissions from subway lines in the planning stage on a city level. *Journal of Cleaner Production.* 2020;259.
40. Liu M, Zhang X, Zhang M, Feng Y, Liu LJEIAR. Influencing factors of carbon emissions in transportation industry based on CD function and LMDI decomposition model: China as an example. 2021;90(1):106623.
41. Liu S, Shen J, Liu G, Wu Y, Shi K. Exploring the effect of urban spatial development pattern on carbon dioxide emissions in China: A socioeconomic density distribution approach based on remotely sensed nighttime light data. *Computers Environment and Urban Systems.* 2022;96.
42. Lv Q, Liu H, Yang D, Liu H. Effects of urbanization on freight transport carbon emissions in China: Common characteristics and regional disparity. *Journal of Cleaner Production.* 2019;211:481-489.
43. Lv Y, Zhi D, Sun H, Qi G. Mobility pattern recognition based prediction for the subway station related bike-sharing trips. *Transportation Research Part C-Emerging Technologies.* 2021;133.
44. Ma X, Ji Y, Yuan Y, Oort NV, Jin Y, Hoogendoorn S. A comparison in travel patterns and determinants of user demand between docked and dockless bike-sharing systems using multi-sourced data. *Transportation Research Part a-Policy and Practice.* 2020;139:148-173.
45. Mahmoudi R, Rasti-Barzoki M. Sustainable supply chains under government intervention with a real-world case study: An evolutionary game theoretic approach. *Computers Industrial Engineering.* 2018;116:130-143.
46. Mahmoudi R, Shetab-Boushehri S-N, Hejazi SR, Emrouznejad A. Determining the relative importance of sustainability evaluation criteria of urban transportation network. *Sustainable Cities and Society.* 2019;47.
47. Mansourianfar MH, Haghshenas H. Micro-scale sustainability assessment of infrastructure projects on urban transportation systems: Case study of Azadi district, Isfahan, Iran. *Cities.* 2018;72:149-159.
48. Marina Gonzalez R, Marrero GA, Rodriguez-Lopez J, Marrero AS. Analyzing CO2 emissions from passenger cars in Europe: A dynamic panel data approach. *Energy Policy.* 2019;129:1271-1281.
49. Marina Gonzalez R, Marrero GA, Rodriguez-Lopez J, Marrero AS. Analyzing CO₂ emissions from passenger cars in Europe: A dynamic panel data approach. *Energy Policy.* 2019;129:1271-1281.
50. McQueen M, MacArthur J, Cherry C. The E-Bike Potential: Estimating regional e-bike impacts on greenhouse gas emissions. *Transportation Research Part D-Transport and Environment.* 2020;87.
51. Moran PAP. Notes on Continuous Stochastic Phenomena. *Biometrika*. 1950;37:17–23.
52. Nadafianshahamabadi R, Tayarani M, Rowangould GM. Differences in expertise and values: Comparing community and expert assessments of a transportation project. *Sustainable Cities and Society.* 2017;28:67-75.

53. Nanaki EA, Koroneos CJ, Roset J, et al. Environmental assessment of 9 European public bus transportation systems. *Sustainable Cities and Society.* 2017;28:42-52.
54. O'Driscoll C, Crowley F, Doran J, McCarthy N. Retail sprawl and CO2 emissions: Retail centres in Irish cities. *Journal of Transport Geography.* 2022;102.
55. Oses U, Roji E, Cuadrado J, Larrauri M. Multiple-Criteria Decision-Making Tool for Local Governments to Evaluate the Global and Local Sustainability of Transportation Systems in Urban Areas: Case Study. *Journal of Urban Planning and Development.* 2018;144(1).
56. O'sullivan D, Unwin D. *Geographic information analysis.* John Wiley & Sons; 2003.
57. Qiao W, Huang X. How does transportation development affect environmental performance? Evidence from Hainan Province, China. *Cities.* 2022;129:103835.
58. Song W, Zhang X, An K, Yang T, Li H, Wang C. Quantifying the spillover elasticities of urban built environment configurations on the adjacent traffic CO₂ emissions in mainland China. *Applied Energy.* 2021;283.
59. Srejic T, Manojlovic S, Sibinovic M, et al. Agricultural Land Use Changes as a Driving Force of Soil Erosion in the Velika Morava River Basin, Serbia. *Agriculture-Basel.* 2023;13(4).
60. Sun S, Wang Z, Wang W. Dockless or docked: Which bike-sharing mode is more environmentally friendly for the city? Current evidence from China's major cities. *Cities.* 2024;147:104816.
61. Taiebat M, Amini E, Xu M. Sharing behavior in ride-hailing trips: A machine learning inference approach. *Transportation Research Part D-Transport and Environment.* 2022;103.
62. Tu M, Li W, Orfila O, Li Y, Gruyer D. Exploring nonlinear effects of the built environment on ridesplitting: Evidence from Chengdu. *Transportation Research Part D-Transport and Environment.* 2021;93.
63. Ture Y, Ture C. An assessment of using Aluminum and Magnesium on CO2 emission in European passenger cars. *Journal of Cleaner Production.* 2020;247.
64. Wang C, Wood J, Wang Y, Geng X, Long X. CO2 emission in transportation sector across 51 countries along the Belt and Road from 2000 to 2014. *Journal of Cleaner Production.* 2020;266.
65. Wang C, Zhao Y, Wang Y, Wood J, Kim CY, Li Y. Transportation CO2 emission decoupling: An assessment of the Eurasian logistics corridor. *Transportation Research Part D-Transport and Environment.* 2020;86.
66. Xia Y, Liao C, Chen X, et al. Future reductions of China's transport emissions impacted by changing driving behaviour. *Nature Sustainability.* 2023.
67. Xu G, Lv Y, Sun H, Wu J, Yang Z. Mobility and evaluation of intercity freight CO₂ emissions in an urban agglomeration. *Transportation Research Part D-Transport and Environment.* 2021;91.
68. Yang L, Hong S. Impact of the clean energy structure of building operation on the co-benefits of CO2 and air pollutant emission reductions in Chinese provinces. *Journal of Cleaner Production.* 2023;413.
69. Yang T, Shu Y, Zhang S, Wang H, Zhu J, Wang F. Impacts of end-use electrification on air

quality and CO2 emissions in China's northern cities in 2030. *Energy.* 2023;278.
70. Yu X, Liang Z, Fan J, Zhang J, Luo Y, Zhu X. Spatial decomposition of city-level CO2 emission changes in Beijing-Tianjin-Hebei. *Journal of Cleaner Production.* 2021;296.
71. Zhang C, Luo L, Xu W, Ledwith V. Use of local Moran's I and GIS to identify pollution hotspots of Pb in urban soils of Galway, Ireland. *Science of the Total Environment.* 2008;398(1-3):212-221.
72. Zhi D, Sun H, Lv Y, Xu G. Quantifying the comprehensive benefit of the bike-sharing system under cycling behavior differences. *Journal of Cleaner Production.* 2022;379.
73. Zhu C, Du W. A Research on Driving Factors of Carbon Emissions of Road Transportation Industry in Six Asia-Pacific Countries Based on the LMDI Decomposition Method. *Energies.* 2019;12(21).
74. Zhu L. Comparative evaluation of CO2 emissions from transportation in countries around the world. *Journal of Transport Geography.* 2023;110.
75. Bai R, Lam JC, Li VO. What dictates income in New York City? SHAP analysis of income estimation based on Socio-economic and Spatial Information Gaussian Processes (SSIG). Humanities Social Sciences Communications. 2023;10(1):1-14.
76. Biau, G., 2012. Analysis of a random forests model. J. Mach. Learn. Res. 13, 1063–1095.
77. Yan, X., Liu, X., Zhao, X., 2020. Using machine learning for direct demand modeling of ridesourcing services in Chicago. Journal of Transport Geography 83, 102661.
78. Breiman, L., 2001. Random forests. Mach. Learn. 45, 5–32.
79. Pedregosa, F., Varoquaux, G., Gramfort, A., Michel, V., Thirion, B., Grisel, O., Blondel, M.,Prettenhofer, P., Weiss, R., Dubourg, V., et al., 2011. Scikit-learn: machine learning in python. J. Mach. Learn. Res. 12, 2825–2830.
80. Molnar, C., 2020. Interpretable machine learning: A guide for making black box models explainable.
81. Wang F, Fan W, Liu J, et al. The effect of urbanization and spatial agglomeration on carbon emissions in urban agglomeration[J]. Environmental science and pollution research, 2020, 27: 24329-24341.
82. Liu D, Xiao B. Can China achieve its carbon emission peaking? A scenario analysis based on STIRPAT and system dynamics model[J]. Ecological indicators, 2018, 93: 647-657.
83. Qian Y, Wang H, Wu J. Spatiotemporal association of carbon dioxide emissions in China's urban agglomerations[J]. Journal of Environmental management, 2022, 323: 116109.
84. Qiao Q, Eskandari H, Saadatmand H, et al. An interpretable multi-stage forecasting framework for energy consumption and CO2 emissions for the transportation sector[J]. Energy, 2024, 286: 129499.
85. Ağbulut Ü. Forecasting of transportation-related energy demand and CO2 emissions in Turkey with different machine learning algorithms[J]. Sustainable Production and Consumption, 2022, 29: 141-157.
86. Sahraei M A, Çodur M K. Prediction of transportation energy demand by novel hybrid meta-heuristic ANN[J]. Energy, 2022, 249: 123735.
87. Javanmard M E, Tang Y, Wang Z, et al. Forecast energy demand, CO2 emissions and energy resource impacts for the transportation sector[J]. Applied Energy, 2023, 338: 120830.

88. Khajavi H, Rastgoo A. Predicting the carbon dioxide emission caused by road transport using a Random Forest (RF) model combined by Meta-Heuristic Algorithms[J]. Sustainable Cities and Society, 2023, 93: 104503.
89. Wang L, Wu Z, Wang X. Multimodal transportation and city carbon emissions over space and time: Evidence from Guangdong-Hong Kong-Macao Greater Bay Area, China[J]. Journal of Cleaner Production, 2023, 425: 138987.